TENM4 is an essential transduction component for touch and pain

Mohammed A. Khallaf[1,2], Angela Tzu-Lun Huang[1], Letizia Dalmasso[1], Sampurna Chakrabarti[1], Rowena Groeneveld[1], Yinth Andrea Bernal Sierra[1], Jonathan Alexis Garcia-Contreras[1], Anja Schütz[3], Valérie Bégay[1], Sarah Hedtrich[4,5,6,7], Wei Zhong[1], Oliver Popp[5], Philipp Mertins[5], and Gary R. Lewin[1,9,10*]

[1]Max Delbrück Center for Molecular Medicine in the Helmholtz Association (MDC), Molecular Physiology of Somatic Sensation, Robert-Rössle Str. 10, 13125 Berlin-Buch, Germany

[2]Department of Zoology and Entomology, Faculty of Science, Assiut University, Assiut, 71516 Egypt

[3]Max Delbrück Center for Molecular Medicine in the Helmholtz Association (MDC), Protein Production and Characterization, Robert-Rössle Str. 10, 13125 Berlin-Buch, Germany

[4]Berlin Institute of Health at Charité - Universitätsmedizin Berlin, Germany Charité – Universitätsmedizin Berlin, Germany

[5]Department of Infectious Diseases and Respiratory Medicine, Charité - Universitätsmedizin Berlin

[6]Faculty of Pharmaceutical Sciences, The University of British Columbia, Vancouver, BC, Canada

[7]Max-Delbrück Center for Molecular Medicine in the Helmholtz Association (MDC), 13125 Berlin, Germany

[8]Max Delbrück Center for Molecular Medicine in the Helmholtz Association (MDC), Proteomics, Robert-Rössle Str. 10, 13125 Berlin-Buch, Germany

[9]Charité-Universitätsmedizin Berlin, Charitéplatz 1, 10117 Berlin, Germany

[10]German Center for Mental Health (DZPG), partner site Berlin

*Correspondence glewin@mdc-berlin.de

Abstract

A gentle touch or a painful pinch are relayed to the brain and spinal cord by rapidly conducting myelinated sensory neurons[1,2]. These sensory neurons possess mechanically activated ion channels like PIEZO2 and ELKIN1 that can be gated by small movements of the substrate[3–6]. This gating mechanism has been proposed to involve extracellular tether proteins that may transfer force from the matrix to the channel[7], the so-called force from tether model[8]. The molecular nature of such tethers has, however, remained elusive. Here we identify the type II membrane protein Teneurin-4 (TENM4) as an essential component for mechanosensory transduction in the vast majority of cutaneous mechanoreceptors, including fast conducting nociceptors. Sensory neuron specific genetic ablation of *Tenm4* in mice led to profound touch insensitivity. We devised a strategy to rapidly and reversibly disassemble the TENM4 protein at sensory endings, demonstrating its direct involvement in sensory transduction. TENM4 has been primarily studied in the context of neural development, but here we provide evidence that it transfers force to mechanically activated channels like PIEZO2 and ELKIN1, with which it associates. The identification of TENM4 as an essential component of fast somatic sensation including fast mechanical nociception is a major step towards identifying treatments for sensory disorders including pain.

Introduction

All organisms, from bacteria to humans, react within a fraction of a second to mechanical signals[8,9]. In all branches of life, a molecularly diverse range of mechanosensitive ion channels are rapidly gated by force to initiate signaling[8]. The fastest and most sensitive mechanosensitive channels detect nanometer scale movements that enable hearing and touch perception[3,4,10]. Interestingly, mechanosensitive channels in fruit flies, worms and vertebrate hair cells all require extracellular proteins that relay force to the channel[10–13]. Vertebrate touch sensation also requires mechanosensitive ion channels, of which PIEZO2 and ELKIN1 share roles in mechanosensation[3,5]. The skin is supplied with a rich variety of molecularly and physiologically distinct mechanoreceptors[2,14], the cell bodies of which reside in the dorsal root ganglia (DRG). Despite their functional diversity, all mechanoreceptors transduce mechanical stimuli into electrical signals at specialized neuroglial endings in the skin[15–17]. There are several lines of evidence that extracellular proteins at these neuroglial endings are directly involved in transferring force to mechanically gated channels[3,5,18–20]. First, mechanically activated currents in sensory neurons can be acutely ablated by proteases, including blisterase, an enzyme that specifically cleaves furin consensus sites[7,16,21]. Mechanosensitive currents are restored 24 hours after protease treatment in cultured sensory neurons, suggesting that the protease target is synthesized by sensory neurons[7]. In the skin, protease treatment of the receptive fields of individual mechanoreceptors rapidly abolishes mechanosensitivity indicating an effect at the neuroglial ending[7]. Protease treatment was also associated with the loss of tether-like structures synthesized by sensory neurons[7]. These data, although suggestive, did not identify the molecular nature of the extracellular protein(s) that are necessary for transduction. Here, we identify TENM4 as a likely tether component necessary for transduction in the vast majority of cutaneous mechanoreceptors.

Screening for tether candidates

Blisterase cleaves a furin consensus site RX(K/R)R which was predicted to occur in at least 11,302 mouse proteins; but only a small minority of these possess putative cleavage sites located in protease accessible extracellular domains. Candidates with predicted extracellular domains were selected using the Database for Annotation, Visualization, and Integrated Discovery (DAVID)[22,23]. Using gene paint[24] (www.genepaint.org) we selected 34 of these genes for further analysis based on the presence of in situ hybridization signals in the developing and adult DRG. Sympathetic neurons located in the superior cervical ganglion (SCG) do not possess mechanically activated currents (MA currents)[7,25]. We thus reasoned that our candidate(s) should be expressed in the DRG, but not in the SCG. Using qPCR, we could not detect the mRNA for six of the 34 genes in the SCG, but all showed robust mRNA expression in the DRG (Extended Data Table 1). The six genes coded for the following proteins; Teneurin-4 (TENM4), FRAS1 Related Extracellular Matrix Protein 2 (FREM2), Proprotein Convertase Subtilisin/Kexin Type 5 (PCSK5), Scribble Homolog (SCRIB), Alpha-Tectorin (TECTA), and Slit Guidance Ligand 1 (SLIT1). We used antibodies directed against the six candidates and obtained signals in cultured DRG neurons for each candidate, but not in SCG cultures, validating the results of the qPCR experiment (Extended Data Fig. 2a). We chose to study TENM4 and FREM2 first, partly because these proteins had the largest extracellular domains of the candidates (mouse proteins 2771 aa and 3160 aa, respectively), consistent with the large tether structures we had previously observed[7,26]. We generated two mouse strains with floxed *Frem2* and *Tenm4* alleles as both *Frem2* and *Tenm4* appear to be essential genes during embryonic development[27,28].

Sensory neuron specific conditional knockouts were created using an adeno-associated virus that is neurotropic for DRG neurons carrying a Cre/GFP cassette (AAV-PHP.S-Cre-eGFP) [29,30]. We examined *Frem2*$^{fl/fl}$ mice 6 weeks after virus application a time point that coincides

with the peak of Cre-mediated excision[30] (*Frem2*^{cko} mice, Extended Data Fig. 1a). However, paw withdrawal thresholds to von Frey hair stimulation, responses to cotton swab and brush stimuli indicated no loss of touch sensitivity in these mice (Extended Data Fig. 2b). We thus turned our attention to the potential role of TENM4 in sensory mechanotransduction.

Mechanoreceptors express the TENM4 protein

TENM4 is a member of the Teneurin family, consisting of four proteins in vertebrates, which are evolutionarily conserved type II membrane proteins known to be essential during neural development[31,32]. Teneurins are dimeric proteins and there is even evidence that hetero-dimers between two different Teneurin proteins may be formed[33]. We identified a commercially available TENM4 antibody directed against the intracellular N-terminus, which is divergent between the four mouse Teneurins (Anti-TENM4-N)[34]. But we also generated an antibody against a large recombinant extracellular fragment which included the extracellular compact YD shell region of the protein (Anti-TENM4-C)[35]. We first looked for TENM4 at the neuroglial endings of a variety of mechanoreceptors types in the skin where touch stimuli are transduced[15,16] (Fig. 1a), and found strong immunolabeling of sensory endings that were also positive for neurofilament-200 (NF200^{+}), a marker of all myelinated sensory fibers (Fig. 1b,c). Sensory endings in end-organs innervated by rapidly adapting mechanoreceptors (RAMs) like Meissner corpuscles, hair follicles, and D-hair receptors were all strongly positive for TENM4 (Fig. 1b). In hair follicles, TENM4 was co-localized with NF200 at lanceolate and circumferential endings around guard and D-hairs (Fig. 1b). Antibodies against S100β were used to label terminal Schwann cells that make up the Meissner corpuscle and are closely associated with lanceolate endings around hair follicles[15,36], however TENM4 labelling was not seen in these cells (Fig. 1b). We found that slowly-adapting mechanoreceptors (SAMs) positive for NF200^{+} that innervate CK20^{+} Merkel cells were also co-labelled with TENM4 (Fig. 1c). Using the same strategy as for *Frem2*, we

generated mice with a sensory neuron specific deletion of *Tenm4* (*Tenm4*^{cko} mice) and saw essentially no TENM4 labeled sensory endings associated with RAM or SAM innervated end-organs (Fig. 1b,c), demonstrating the specificity of the antibody. We also detected TENM4^{+} axons in wild type (WT) skin that appeared to terminate as free nerve endings (Extended Data Fig. 3a). Thus, TENM4 appeared to be a surprisingly good marker of the endings of mouse low threshold mechanoreceptors (LTMRs). We next asked whether sensory endings in human skin could also be labelled with antibodies against TENM4. Human skin from the abdominal region was prepared and subjected to tissue clearing (see Methods). We focused on human hair follicles and found elaborate NF200^{+} lanceolate endings at the base of the follicles, furthermore these endings were all clearly positive for TENM4 (Fig. 1d).

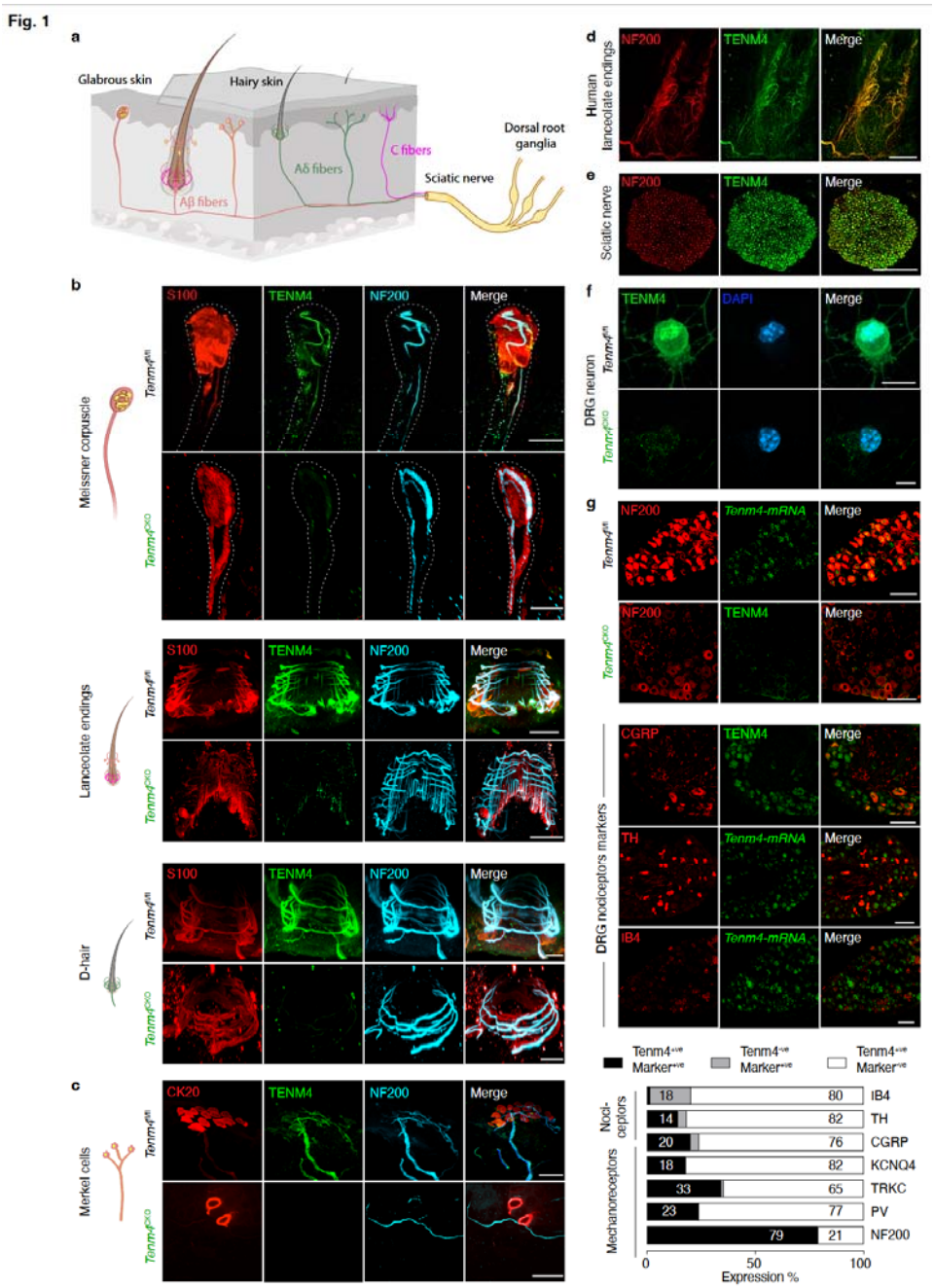

Figure 1

TENM4 is present at sites of transduction in mechanoreceptors. a. Schematic of mechanoreceptor and nociceptor endings in hairy and glabrous skin. **b**. TENM4+ and NF200+ sensory endings associated with rapidly-adapting mechanoreceptors (RAMs) like Meissner's corpuscles, lanceolate endings around hair follicles and D-hair receptors (glabrous footpad)[37]. S100+ terminal Schwann cells were not TENM4+. TENM4 immunostaining was largely absent from RAM endings in *Tenm4*^{CKO} mice. Scale bars 20µm. **c.** Tenm4+ NF200+ endings associated with slowly adapting mechanoreceptors innervating CK20+ Merkel cells in the footpad. TENM4 immunostaining was absent in *Tenm4*^{CKO} mice. Scale bars 20µm. **d**. Lanceolate endings around hair follicles in abdominal

human skin were TENM4+. Scale bar 100μm. **e**. TENM4+ myelinated fibers within the sciatic nerve. Scale bar 50μm. **f**. TENM4+ cultured mouse DRG neuron, staining was absent in cells from *Tenm4*^{CKO} mice. Scale bar 10μm. **g**. Representative DRG sections showing double labelling of DRG section with Tenm4 smFISH probe or TENM4 antibody with NF200, CGRP, TH or IB4, Scale bar 100μm. Bottom shows quantification Tenm4+ sensory neurons co-labeled with deferent sensory markers. For each co-labelling 2 male and 3 female mice were used and more than 700 neurons counted. Note absence of TENM4+ DRG cells in sections from *Tenm4*^{CKO} mice, NF200 staining was unchanged, scale bar 100μm.

Our validated antibody revealed the presence of TENM4 in the myelinated fibers of the sciatic nerve (Fig. 1e) and in large diameter DRG neurons in culture as well as in sections (Fig. 1f,g). We examined *Tenm4*$^{+}$ expression in cells with single molecule fluorescence hybridization (smFISH), and examined co-labelling with antibodies against markers of nociceptors and mechanoreceptors in DRG sections (Fig. 1g, and Extended Data Fig. 3b-e). Consistent with our results from the skin, all NF200^{+} cells were also *TENM4*$^{+}$, but we saw very little, or no overlap with nociceptor markers such as isolectin-B4 (IB4)[38] (Fig. 1g). However, many nociceptive sensory neurons positive for calcitonin-gene related peptide (CGRP) were also co-labeled with the TENM4 antibody (Fig. 1g). Small sensory neurons positive for tyrosine hydroxylase (TH), a marker of low threshold tactile C-fibers, were also largely positive for *Tenm4* mRNA. *Kcnq4* expression is highly specific to RAMs[39] and all these cells were also positive for *Tenm4* mRNA (Fig. 1g, Extended Data Fig. 3g). We carried out immunostaining of TENM4 in the DRG and noted that the signal was largely absent in sections or cultured sensory neurons from *Tenm4*^{CKO} mice (Fig. 1f, h). Together, these data indicate that TENM4 is selectively present in virtually all mechanoreceptors including nociceptors with myelinated axons, suggesting its involvement in mammalian touch and pain sensation.

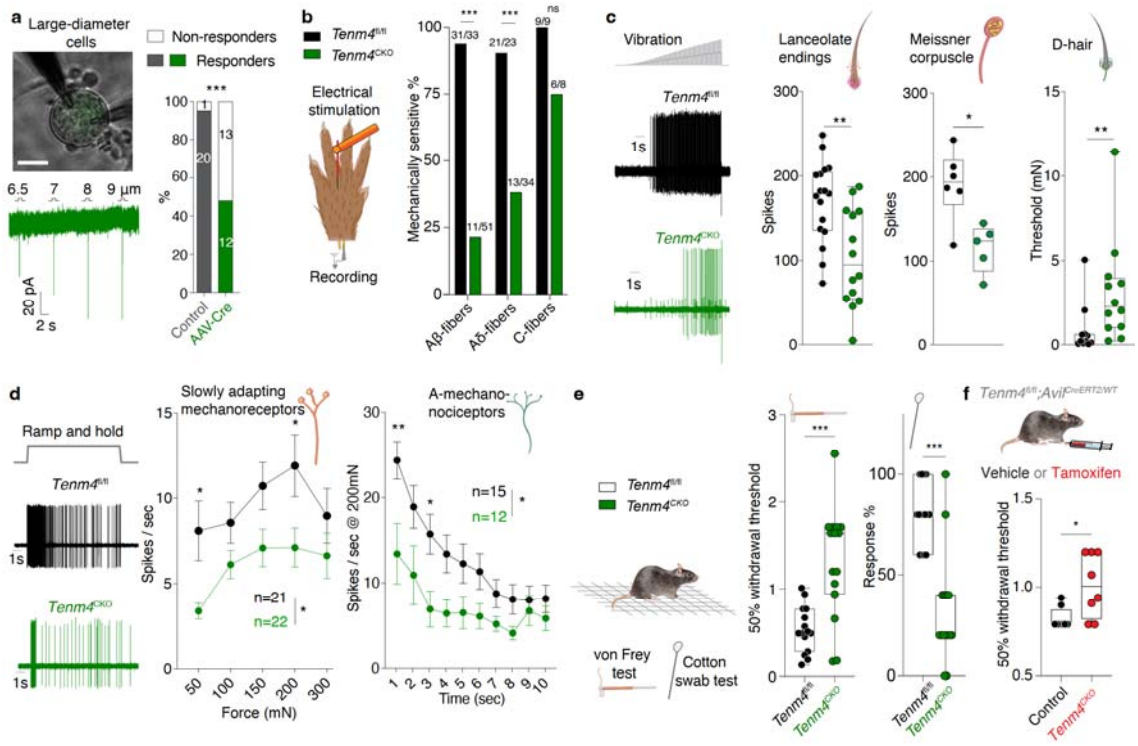

Figure 2

TENM4 is required for mechanoreceptor function and touch sensation. **a**. Poking-induced currents in GFP positive sensory neurons infected with the AAV-PHP.S-Cre-EGFP. Scale bar 20µm. *Tenm4*^{CKO} mice had a deficit in MA-currents in large neurons compared to control *Tenm4*$^{fl/fl}$ mice. Significance calculated with Chi-squared test. Data collected from 4 *Tenm4*$^{fl/fl}$ and 5 *Tenm4*^{CKO} mice. **b**. Electrical search technique (schematic) used to identify saphenous fibers with and without a mechanosensitive receptive field. *Tenm4*^{CKO} mice exhibited a substantial increase in Aβ-fibers and Aδ-fibers without a mechanosensitive receptive field, C-fibers remained unaffected. Significance calculated with Fisher's exact test, data from 5 *Tenm4*$^{fl/fl}$ (control) and 7 *Tenm4*^{CKO} mice. **c**. Example traces of vibration sensitive RAMs. Firing to vibration stimuli in RAMs associated with hairs or Meissner's corpuscles in *Tenm4*^{CKO} mice were significantly reduced. RAM Aδ-fibers innervating D-hairs in *Tenm4*^{CKO} mice exhibited significantly higher mechanical thresholds compared to control mice. Significance calculated with Mann-Whitney test. **d**. Example SAM responses to a 50 mN amplitude ramp and hold stimulus. Stimulus response functions of SAMs were significantly impaired in *Tenm4*^{CKO} mice. Additionally, Aδ-mechanonociceptors showed reduced firing during a 10s long 200 mN stimulus compared to control mice. Significance calculated with two-way repeated measures ANOVA followed by Sidak's post-hoc tests. Data collected from 6 *Tenm4*$^{fl/fl}$ and 9 *Tenm4*^{CKO} mice. **e**. Behavioral tests on touch evoked behaviors. *Tenm4*^{CKO} mice exhibited three-fold higher withdrawal thresholds and significant deficits in mean force required for a 50% withdrawal using von Frey hairs, compared to controls. Additionally, *Tenm4*^{CKO} mice exhibited reduced responses to a cotton swab and a dynamic brush. Data were collected from 15 *Tenm4*$^{fl/fl}$ and 15 *Tenm4*^{CKO} mice. Significance calculated with Student's T-Test. **f.** *Tenm4*$^{fl/fl}$*; Avil*$^{CreERT2/WT}$ mice were used to achieve tamoxifen induced sensory neuron specific *Tenm4* deletion. *Tenm4*^{CKO} mice exhibited significantly higher withdrawal thresholds to von Frey stimuli compared to control mice. Data were collected from 8 control and 8 *Tenm4*^{CKO} mice. * $p < 0.05$; ** $p < 0.01$; ***; $p < 0.001$, means ± s.e.m.

Sensory neuron specific *Tenm4* gene deletion abolishes mechanosensitivity

Cultured large diameter sensory neurons possess sensitive and large amplitude indentation-induced currents that are also abolished after protease treatment[5,7,40]. We made whole cell patch clamp recordings and measured MA currents in isolated large sensory neurons (diameter >30μm) using cell indentation (Fig. 2a). Almost all large neurons from control mice positive for GFP (*Tenm4*$^{fl/fl}$ injected with AAV-PHP.S-eGFP virus, lacking Cre) displayed robust MA currents (Fig. 2a). In contrast, over half of the large diameter GFP-positive neurons recorded from *Tenm4*^{CKO} mice lacked any MA current (Fig. 2a, Extended Data Fig 4a). However, the incidence and characteristics of MA currents recorded from small diameter sensory neurons were comparable between neurons from *Tenm4*^{CKO} mice and controls (Extended Data Fig. 4b).

The absence of MA currents in cultured DRG neurons has been consistently associated with an effective silencing of mechanoreceptors in the skin [3,5,18–20]. We used an ex vivo saphenous skin-nerve preparation to trace the trajectory of single units by means of an electrical stimulus until the point of exit from the nerve branch. Normally, single identified Aβ- and Aδ-fibers always have a mechanosensitive receptive field in the skin near to the nerve exit point[3,5,19,41], which we confirmed here in control mice (*Tenm4*$^{fl/fl}$) (Fig. 2b). However, blinded recordings made from *Tenm4*^{CKO} mice revealed that 75% of the Aβ-fibers and 60% of Aδ-fibers had no detectable mechanosensitive receptive field (Fig. 2b). Recordings from C-fiber nociceptors revealed no significant differences in the presence of mechanosensitive receptive fields between control and *Tenm4*^{CKO} mice (Fig. 2b).

We next analyzed the stimulus response characteristics of the remaining non-silenced sensory fibers identified using a mechanical search stimulus in both glabrous and hairy skin[37,42]. We used a 20Hz vibrating stimulus with continuously increasing amplitude to stimulate RAMs in hairy and glabrous skin. We found that all RAMs displayed significantly reduced firing rates in *Tenm4*^{CKO} mice compared to control mice (Fig. 2c). Velocity sensitivity was also measured

using ramp stimuli of different velocities and spike rates to these stimuli were also significantly impaired in RAMs from *Tenm4*^{CKO} mice (Extended Data Fig. 5f). Low threshold mechanoreceptors with Aδ-fiber conduction velocities, so called D-hair receptors, showed significantly higher vibration thresholds in *Tenm4*^{CKO} mice compared to controls (Fig. 2c, Extended Data Fig. 5e). Merkel cells are innervated by slowly adapting mechanoreceptors (SAMs) and are found in hairy and glabrous skin. Stimulus response functions calculated with a series of 10s long ramp and hold stimuli showed that SAMs fired significantly less and had higher mechanical thresholds for activation in *Tenm4*^{CKO} mice compared to controls (Fig 2d, Extended Data 5e). We also recorded from Aδ mechanonociceptors (AMs) which detect sustained high threshold mechanical stimuli and contribute to fast mechanical pain sensation[1,2]. In *Tenm4*^{CKO} AMs displayed significantly reduced sustained firing to high forces and stimulus response functions were reduced, but this was not significantly different compared to controls (Fig. 2d, Extended Data Fig. 5g). Taken together, our data show that TENM4 is absolutely necessary for the mechanosensory function of almost all cutaneous sensory receptors, likely because the protein is required the function of MA currents in these neurons.

Profound sensory deficits in *Tenm4*^{cko} mice

Tenm4^{CKO} mice animals displayed substantially reduced responses to a cotton swab and dynamic brush stimuli (Fig. 2e, Extended Data Fig. 6a). Additionally, paw withdrawal thresholds to a series of von Frey hairs were substantially elevated in *Tenm4*^{CKO} mice (Fig. 2e, Extended Data Fig. 6a). Expression of the GFP marker in sensory neurons indicated that >80% of the cells were transduced (Extended Data Fig. 5a). Sensory deficits varied in degree between individuals probably due to differences in the efficiency of viral transduction and gene excision, but in many cases, animals completely failed to respond to mechanical stimuli indicating a profound loss of sensation (Fig 2e; Extended Data Fig. 6a). Importantly, we

observed no changes in axonal morphology or number in *Tenm4*^{CKO} mice using transmission electron microscopy (Extended Data Fig. 5b).

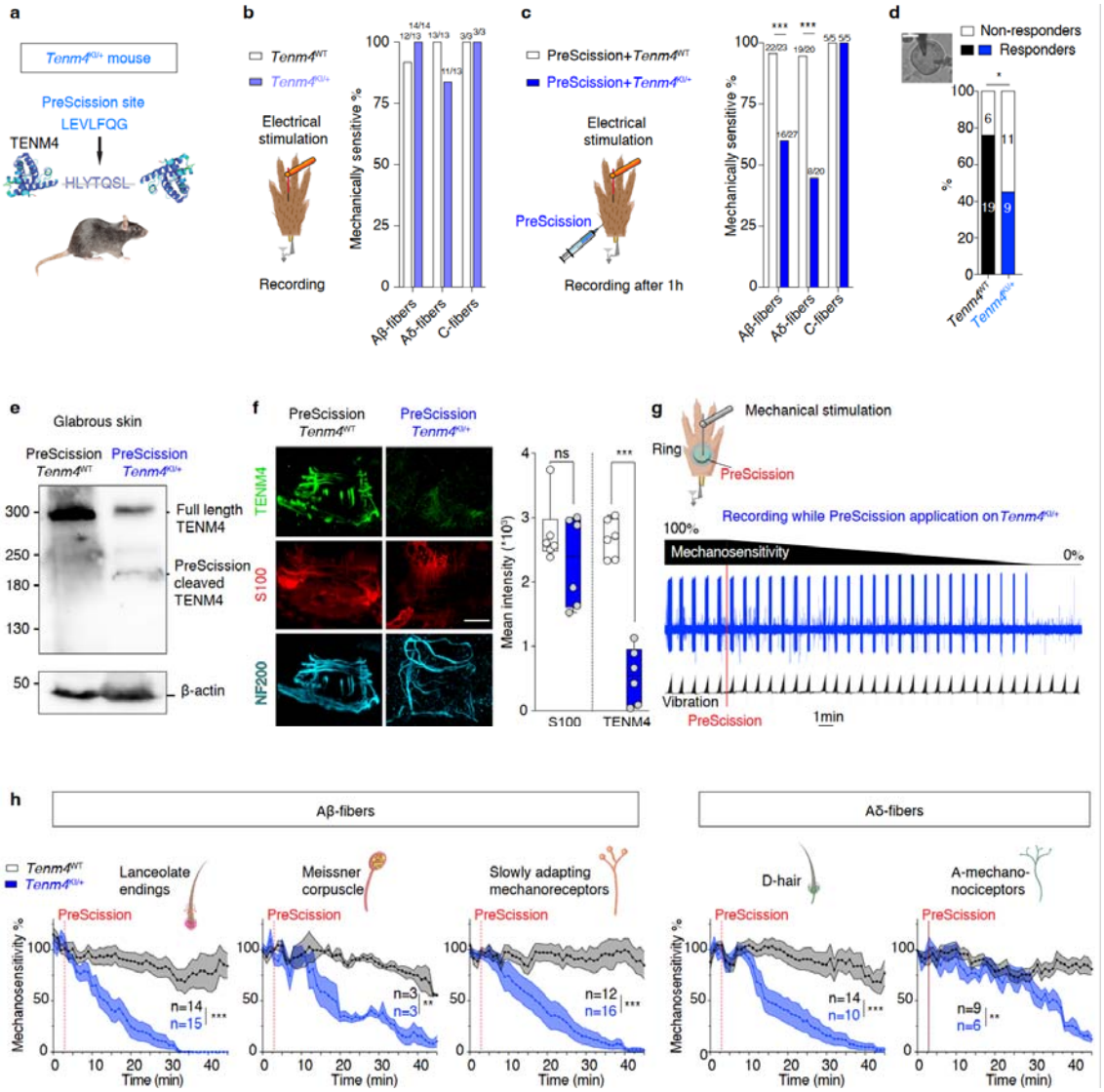

Figure 3

Rapid loss of mechanoreceptor function following TENM4 cleavage. a. Generation of *Tenm4*$^{KI/+}$ mice: insertion of a 7 residue PreScission consensus sequence into genomic locus encoding the TENM4 extracellular domain. **b**. Electrical search technique revealed that most Aβ, Aδ, and C-fibers retained mechanosensitivity in *Tenm4*$^{KI/+}$ mice as in WT mice. Significance calculated with Fisher's exact test. Data collected from 4 WT (control) and 5 *Tenm4*$^{KI/+}$ mice. **c**. Electrical search 1 hour after PreScission protease injections. Substantial and significant decrease in the proportion of Aβ and Aδ-fibers displaying mechanosensitivity in PreScission treated *Tenm4*$^{KI/+}$, but not in WT mice. The proportion of mechanosensitive C-fibers remained unchanged in both groups. Significance calculated with Fisher's exact test. Data collected from 4 WT and 4 *Tenm4*$^{KI/+}$ mice. **d**. Recordings from large diameter sensory in culture (scale bar = 20μm) showed a substantial decrease in the proportion of

cells with poking-induced currents, specifically in cells from *Tenm4*$^{KI/+}$ treated with the PreScission protease. Significance calculated with Chi-squared test. **e**. Western blot of endogenous TENM4 from glabrous skin after PreScission protease treatment revealed uncleaved full-length TENM4 in WT mice, a cleaved product of the predicted size was detected in *Tenm4*$^{KI/+}$ mice. Loading control β-actin. **f**. Representative images and quantitative analysis of the specific loss of TENM4 immunostaining of lanceolate endings following PreScission protease treatment of skin from *Tenm*$^{KI/+}$ mice. In contrast, TENM4 immunostaining was unchanged after PreScission treatment of WT skin. Scale bar 20μm. **g**. Representative example of a single unit (RAM) responding to repeated 20Hz vibration before and after application of PreScission to the receptive field in a *Tenm4*$^{KI/+}$ mouse. Note the progressive decrease in stimulus induced firing following PreScission treatment. **h.** Mean mechanoreceptor responses plotted as a percentage of the starting value for all myelinated Aβ and Aδ fiber types, before and after PreScission. Note mechanoreceptors in WT all retained mechanosensitivity (grey), but all mechanoreceptor types in *Tenm4*$^{KI/+}$ mice, progressively lost responsiveness during the 45 mins of observation (blue) * $p < 0.05$; ** $p < 0.01$; ***; $p < 0.001$, means ± s.e.m.

We confirmed these results using a complementary strategy in which we generated mice where the *Tenm4*$^{fl/fl}$ alleles were crossed with mice carrying an *Advillin-CreERT2* allele allowing the inducible deletion of *Tenm4* only in sensory neurons following tamoxifen treatment. Around 4 weeks after tamoxifen injections *Tenm4*$^{fl/fl}$*:Avil*^{CreERT2} mice were tested for paw withdrawal using a series of von Frey hairs of increasing force. As for virus injected mice, these treated animals displayed profoundly elevated paw withdrawal thresholds (Fig. 2f). Using a radiant heat stimulus we measured thermal thresholds in both *Tenm4*$^{fl/fl}$*:Avil*^{CreERT2} and virus injected *Tenm4*^{CKO} mice and found no significant deficits. Thus, the sensory deficits we observed after ablation of *Tenm4* in sensory neurons were highly specific to mechanical stimuli (Extended Data Fig. 6b,c).

TENM4 cleavage rapidly abolishes mechanosensitivity

Cre-mediated excision using AAV vectors leads to the removal of *Tenm4* over several weeks. TENM4 is potentially involved in intercellular signaling[34,35], the alteration of which could have indirect effects on transduction. Therefore, we wished to directly test the idea that TENM4 forms part of a transduction complex that facilitates force transfer from the extracellular matrix (ECM) to transduction channels. Ideally, specific cleavage of proteins linking the channel to ECM should abolish transduction. We thus developed a new

technology that enabled us to specifically ablate TENM4 function within minutes. We named this method PreScission Protein Disassembly, and it is based on the fact that the plant virus derived PreScission protease cleaves a specific consensus sequence (LEVLFQ↓GP)[43] that rarely occurs in the extracellular exposed residues of mouse proteins (Extended Data Table 2). Using homologous recombination in mouse ES cells we inserted the PreScission cleavage sequence into *Tenm4*. In this case we replaced 9 codons leading to the replacement of 7 amino acids which expose a PreScission sequence on the surface of the extracellular YD shell domain of TENM4[35]. This manipulation was predicted to make TENM4 newly susceptible to cleavage by the PreScission enzyme (Fig. 3a, and Extended Data Fig. 1c). Mice carrying the PreScission site in the *Tenm4* gene were bred, but out of 569 newborns from heterozygote crosses we obtained no homozygote animals. The failure to obtain homozygotes indicates that altering both *Tenm4* alleles likely causes embryonic lethality, consistent with previous studies[34,44]. We thus decided to work with heterozygotes which we termed $Tenm4^{KI/+}$ mice. Assuming that TenM4 forms homodimers[33], a stochastic mixing of mutated and wild type proteins would ensure that the vast majority of dimers would have at least one PreScission cleavable site. Considering the observed embryonic lethality, it was important to examine whether $Tenm4^{KI/+}$ mice show deficits in baseline sensory function. $Tenm4^{KI/+}$ mice showed no deficits in behavioral responses to mechanical and thermal stimuli (Extended Data Fig. 7). We also made recordings from the saphenous nerve of $Tenm4^{KI/+}$ mice and, using the electrical search method, demonstrated that Aβ-fibers, Aδ-fibers and C-fibers exhibited normal mechanosensitivity, with unaltered stimulus response properties and normal axonal conduction velocities (Fig. 3b, and Extended Data Fig. 8). We next injected the PreScission protease (2 units /μL) subcutaneously into the hairy skin innervated by the saphenous nerve. One hour after injection we made ex vivo skin nerve recordings from the saphenous nerve and used the electrical search method to probe how many sensory fibers have

mechanosensitive receptive fields. *Tenm4*$^{KI/+}$ mice, but not treated *Tenm4*^{wt}, exhibited a substantial and significant decrease in the proportion of Aβ and Aδ-fibers with a mechanosensitive receptive field. No loss of C-fiber mechanosensitivity was observed in either genotype treated with the PreScission protease (Fig. 3c). In parallel we made whole cell patch clamp recordings from cultured DRG neurons. Here, a substantial proportion of PreScission-treated large-diameter DRG neurons in *Tenm4*$^{KI/+}$ showed no MA current which was significantly different from WT treated neurons (Fig. 3d, and Extended Data Fig. 9a). In summary, treatment of the skin and cultured sensory neurons with PreScission protease in *Tenm4*$^{KI/+}$ mice led to a similar loss of mechanosensitivity as seen in *Tenm4*^{CKO} mice (Fig. 2b). In order to confirm that the PreScission enzyme actually cleaves TENM4 in vivo, we prepared Western blots from the glabrous skin and could detect a 300 KDa band corresponding to uncleaved TENM4 in WT skin treated with PreScission protease. However, in skin samples taken from *Tenm4*$^{KI/+}$mice, treated with PreScission, we not only detected the full-length protein, but also a ~180 kDa fragment which has the size predicted for the cleavage product (Fig. 3e). The incomplete cleavage is presumably due to the fact that half of the TENM4 present cannot be cleaved by PreScission protease. Next, we used our custom made TENM4-C-terminal antibody which recognizes the extracellular domain of the protein to label sensory end-organs like hair follicles lanceolate endings. Since the extracellular domain is cleaved by PreScission protease, we reasoned that treatment of the skin with the protease should lead to the loss of TENM4 immuno-positive sensory endings. Indeed, we observed a clear loss of TENM4 immuno-stained lanceolate endings after protease treatment (Fig 3f).

We next used acute application of PreScission protease to the receptive fields of single identified mechanoreceptors to examine the kinetics of the protease effect on mechanosensitivity. Once a mechanoreceptor was identified and classified[37], the receptive

field was isolated with a metal ring and repeatedly stimulated every minute for up to 60 mins. We used a vibration stimulus (20Hz gradually increasing to maximum 100 mN amplitude) for all LTMRs (RAMs, SAMs and D-hair receptors) or a 150mN amplitude ramp and hold stimulus for mechanonociceptors (AMs or C-fiber nociceptors). After baseline recordings for three minutes the receptive field was exposed to the PreScission enzyme (2 units/µL) in physiological ringer solution (Fig. 3g). Remarkably, all LTMRs (RAMs, SAMs and D-hair receptors) recorded from *Tenm4*$^{KI/+}$ mice showed progressively decreasing spike responses to the constant mechanical stimuli starting minutes after protease application, until no response was evoked between 30 and 45 minutes. In contrast, protease treated LTMRs from WT mice showed remarkably robust spiking for the entire 45 mins with barely any diminution of mechanosensitivity (Fig. 3h). For each mechanoreceptor examined we used an electrical stimulus at the end of the experiment to show that the spike was still present indicating a specific loss of mechanosensitivity (Fig. 3h). Notably, we observed a slower, but robust loss of the ability of AMs in *Tenm4*$^{KI/+}$ to transduce force, reaching its maximum 45 mins after PreScission application (Fig. 3h). However, in contrast to LTMRs, most AMs retained residual responses to intense mechanical stimuli at the end of the 45-minute observation period (5/6 tested). C-fiber nociceptors in WT and *Tenm4*$^{KI/+}$ mice retained functionality after exposure to PreScission protease (Extended Data Fig. 9b), indicating a fundamentally distinct transduction mechanism in AM nociceptors compared to C-fiber nociceptors.

TENM4 cleavage causes profound sensory deficits

Using electrophysiology, we showed that RAMs innervating Meissner's corpuscles in the glabrous skin are also susceptible to the PreScission protease in *Tenm4*$^{KI/+}$ mice (Fig. 3h). We next asked whether touch evoked behaviors which are routinely measured using stimuli to the glabrous skin are impacted by the PreScission protease. In WT mice PreScission injections into the glabrous skin had no significant impact on paw withdrawal thresholds, cotton swab

or brush responses (Fig. 4a, b). However, *Tenm4*$^{KI/+}$ mice exhibited a substantial and significant increase in paw withdrawal thresholds as well as much reduced responses to cotton swab and brush stimuli (Fig. 4a, b). Noxious heat withdrawal latencies were slightly elevated in *Tenm*$^{KI/+}$ mice after PreScission injection, but this was not significantly different from saline injected controls (Extended Data Fig. 10).

Fig. 4

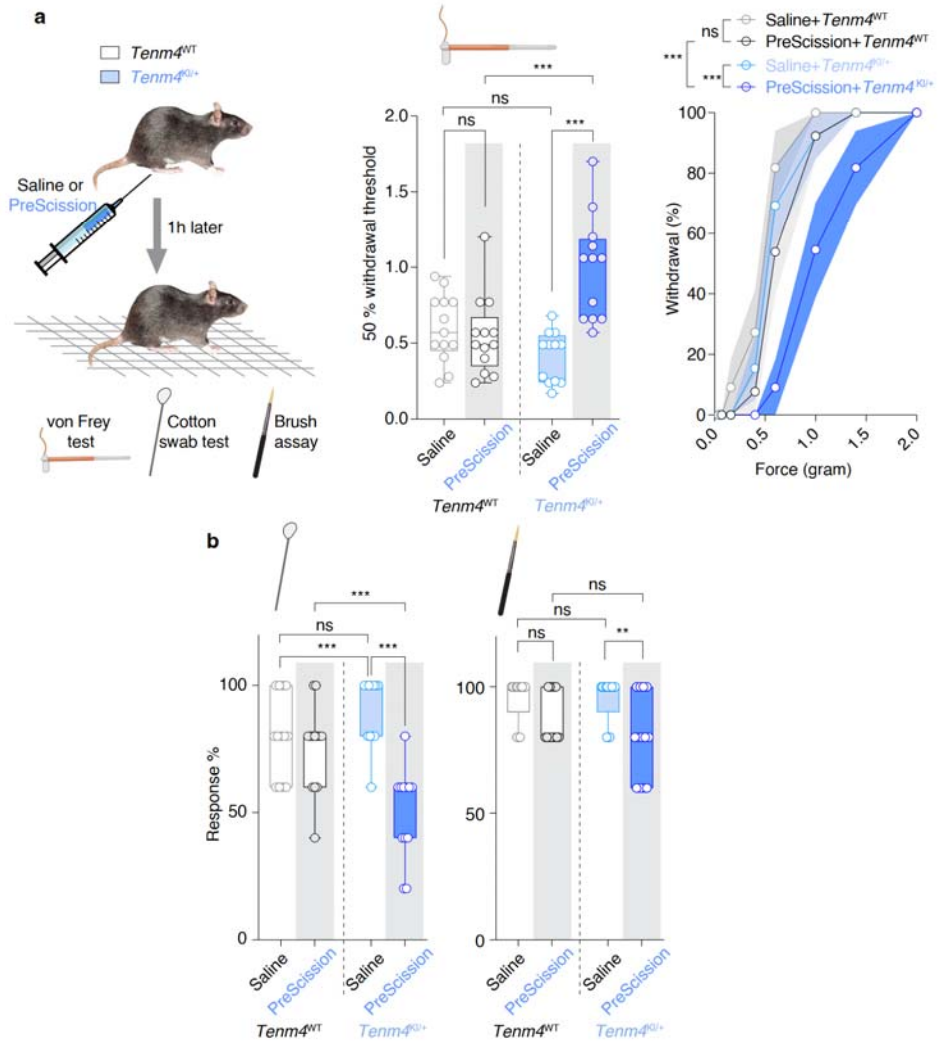

Figure 4

TENM4 cleavage dramatically reduces touch sensitivity. a. Behavioral assays used to assess the effects of TENM4 cleavage 1 hr after PreScission injection to the plantar hind paw. Mechanical withdrawal threshold measured with von Frey hairs were unchanged in WT mice treated with saline or PreScission. Right, the line graph illustrates the mean represented by points and the surrounding

shades indicate s.e.m. A dramatic decrease in sensitivity to von Frey stimulation was observed only after treatment of *Tenm4*$^{KI/+}$mice with PreScission protease, and not with saline. **b.** *Tenm4*$^{KI/+}$ mice injected with PreScission showed decreased responses to both a cotton swab and a dynamic brush, no changes were observed in treated WT mice. Data collected from 13 WT and 12 *Tenm4*$^{KI/+}$ mice. Two-way repeated measures ANOVA followed by Sidak's post-test; ns indicates $p > 0.05$; ** indicates $p < 0.01$; *** indicates $p < 0.001$, means ± s.e.m.

Cleavage of the TENM4 protein clearly leads to an acute loss of touch sensation in *Tenm4*$^{KI/+}$ mice, but in theory the TENM4 protein should be re-synthesized to reinstate function. We thus investigated the temporal dynamics of touch sensation recovery in *Tenm4*$^{KI/+}$ mice following PreScission injections. We found that PreScission-injected *Tenm4*$^{KI/+}$ mice displayed elevated paw withdrawal thresholds at 12, 24, and 48h which had then returned to normal levels at 72h (Fig. 5a). Control WT mice injected with the PreScission protease showed no changes in paw withdrawal thresholds over the same period of time (Fig. 5a). These behavioral changes were likely due to the silencing of Aβ and Aδ-fibers in the injected skin. To test this, we made recordings from electrically isolated single-units and determined how many fibers retained a mechanosensitive receptive field. We found that a substantial proportion of Aβ and Aδ-fibers were still mechanically silent 24h following PreScission injection in *Tenm4*$^{KI/+}$mice. However, at 72h almost all Aβ and Aδ-fibers had mechanosensitive receptive fields, as was observed in PreScission injected WT control mice at 24 and 72h (Fig. 5b). C-fiber nociceptors identified with an electrical search retained normal mechanosensitivity at all time points and conditions (Fig. 5b). Using the TENM4-C-terminal antibody we examined the presence of the protein in sensory endings 24 and 72h following the PreScission injection. We observed much reduced TENM4 immunostaining at 24h, but this had recovered substantially by 72h (Fig. 5c). However, the loss of TENM4 signal was not due to a disintegration of the neuroglial endings as normal NF200^{+} endings were observed at 24h, although the staining intensity was somewhat reduced at 24h but not at 72h. We also observed a normal pattern of S100^{+} terminal Schwann cells associated with the mechanoreceptor end-organs at all points following PreScission treatment (Fig. 5c; Extended

Data Fig. 11). Together, these results reveal that the TENM4 protein is both necessary and sufficient for touch sensation.

Fig. 5

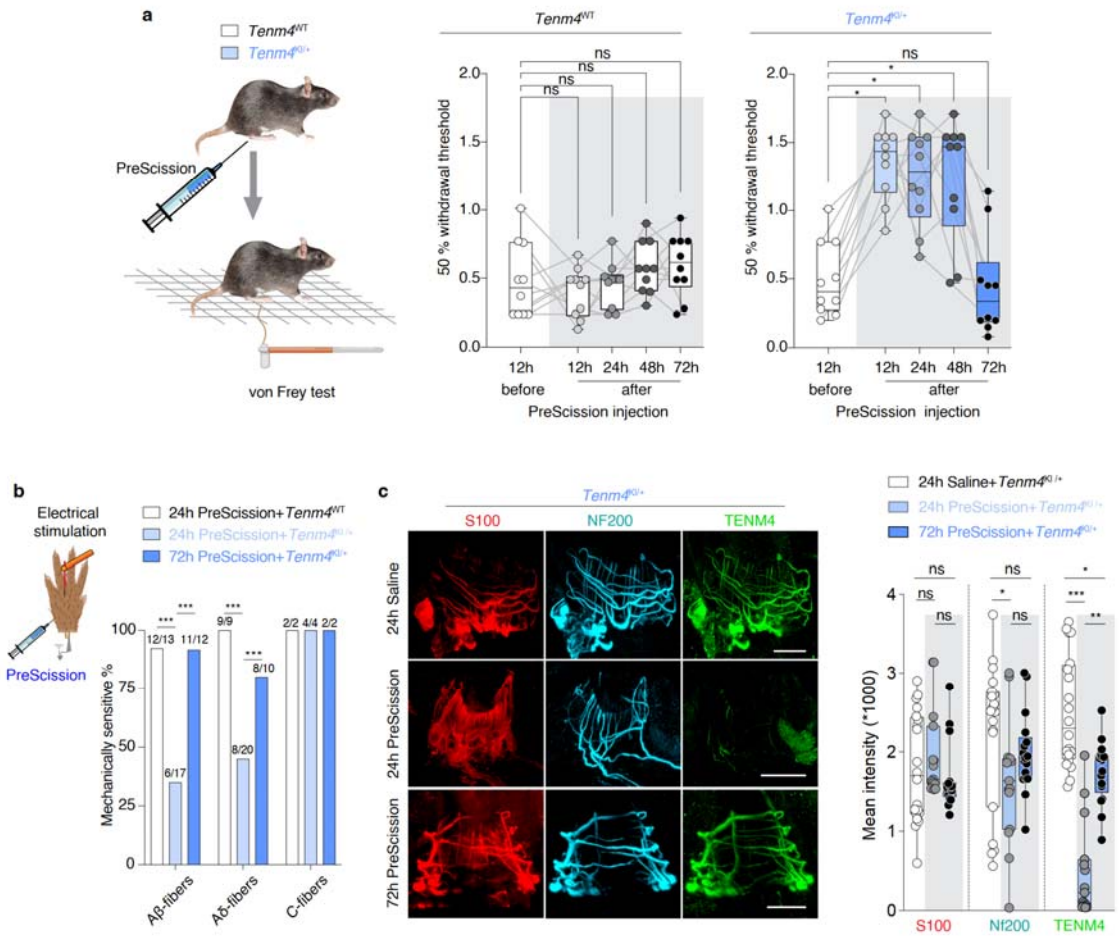

Figure 5

TENM4 is necessary and sufficient for touch sensation. a. Experimental design. WT mice showed constant mean withdrawal thresholds to von Frey filaments before and up to 72h following PreScission treatment. In contrast, PreScission-injected *Tenm4*$^{KI/+}$ mice displayed significantly elevated paw withdrawal thresholds at 12, 24, and 48 hours, which returned to normal by 72h. Statistical significance calculated with Friedman test followed by Dunn's multiple comparisons test. Data collected from 10 mice per group. **b**. Left, electrical search technique conducted 24 or 72h after PreScission protease injection into the hairy skin. Right, *Tenm*$^{KI/+}$ mice exhibit a significant decrease in the proportion of Aβ and Aδ fibers displaying mechanosensitivity only after 24h, but not at 72h, following PreScission injection, while C-fibers remain unaffected at both time points. All WT fibers showed no change. Fisher's exact test. Data were collected from 4 mice per group. **c**. Representative images of TENM4 positive sensory endings and quantitative analysis 24 or 72h after PreScission protease injection into the hairy skin. In *Tenm4*$^{KI/+}$ mice, TENM4+ sensory fibers decrease significantly at 24h, but recovered by 72h, while NF200 and S100 staining remained unchanged at all

time points measured. Data collected from more than 26 samples from 4 mice per group. Statistical significance calculated with Kruskal-Wallis test followed by Dunn's multiple comparisons test. For all tests ns indicates $p > 0.05$; * indicates $p < 0.05$; ** indicates $p < 0.01$; *** indicates $p < 0.001$. means ± s.e.m.

TENM4 associates with mechanically activated ion channels

Our data show that TENM4 is essential for sensory mechanotransduction, but to fulfill this function it must associate with MA channels. MA channels like PIEZO2 and ELKIN1 are efficiently gated by substrate deflection and we asked whether TENM4 can modulate this gating[4–6]. We generated full length *Tenm4* expression constructs with a C-terminal ALFA-tag that can be recognized by fluorescently labeled nanobodies (Extended Data Fig. 12a)[45]. We used Neuro2a-PIEZO1-Knockout (N2a$^{Piezo1\text{-}/\text{-}}$) cells that have minimal, but detectable deflection induced currents[46,47] and transfected these cells with the *Tenm4-Alfa* or control *pRK8-eGFP* constructs. Transfected cells were plated on pillar arrays and then live labelled with anti-ALFA tag nanobodies which bind to the extracellular C-terminus of the expressed TENM4 protein. We made targeted whole cell patch clamp recordings from cells that expressed TENM4 on the membrane and measured the sensitivity and amplitude of currents evoked by single pillar displacements (Fig 6a)[4]. As observed previously, control GFP transfected cells exhibited occasional small amplitude currents to pillar deflection, but we measured a large and significant increase in the frequency and amplitude of currents in cells with plasma membrane-localized TENM4 (Fig. 6a,b). This data suggests that N2a$^{Piezo1\text{-}/\text{-}}$ normally express MA channels that interact with TENM4 to facilitate gating of channels via the extracellular matrix. We therefore carried out a quantitative proteomic analysis of N2a cells to reveal expressed ion channels potentially targeted by TENM4. We compared the proteome of N2a cells with that of N2a$^{Piezo1\text{-}/\text{-}}$ cells and could quantify the levels of more than 8000 proteins in both samples (Extended Data Fig. 13). Interestingly, a large proportion of the

proteome showed significant changes in the absence of PIEZO1, e.g. >16% of the proteome showed significantly higher abundances. Included in the significantly up-regulated protein set were TENM4 itself as well as the MA ion channel ELKIN1/TMEM87A[5,6]. We did not detect any peptides from PIEZO2. Interestingly, many of the highest up-regulated proteins were themselves components of the extracellular matrix (ECM) (Extended Data Fig. 13). This data led us to examine whether TENM4 can associate directly with MA channels like PIEZO2 or ELKIN1[3,5]. Due to the structural similarity among Teneurins, we designed a truncated construct covering the entire N-terminus and a portion of the extracellular region including sequences involved in dimerization to assess binding between Teneurin family members[35]. Utilizing a tripartite-GFP-based protein complementation assay[5], we confirmed that the Teneurins can interact with each other (Extended Data Fig. 12b) [33,48]. We also measured a robust complementation signal (GFP fluorescence) between ELKIN1 and TENM4, and the strength of the interaction signal was notably much higher than that observed for ELKIN1 with other Teneurins (Fig. 6d, and Extended Data Fig. 13c). We next asked whether TENM4 is associated with MA channels on the plasma membrane using Airyscan super-resolution microscopy[49]. We co-expressed our ALFA-tagged *Tenm4* construct with either mScarlet tagged Elkin1 or Piezo2 constructs[50]. Nanobody labeled TENM4 exhibited a punctate distribution on the plasma membrane as did mScarlet tagged PIEZO2 or ELKIN1 (Fig. 6e). Quantification indicated that approximately 75% of TENM4 was colocalized with ELKIN1, while around 30% of TENM4 localized together with PIEZO2 channels (Fig. 6e). Since ELKIN1 channels appeared to best co-localize with TENM4, we designed a biochemical assay to detect ELKIN1/TENM4 complexes. We used HEK-293 cells transfected with *Elkin1* expression plasmids alone or together with ALFA-tagged *Tenm4*. We used ALFA nanobody conjugated resins (ALFA SelectorPE™) to pull down the expressed TENM4 protein complexes which were then eluted using high concentrations of the purified ALFA peptide[45].

Using Western blotting, we could detect co-elution of ELKIN1 specifically in cases where TENM4-ALFA protein had been expressed (Fig. 6f). Together, these results demonstrate specific and direct interactions between TENM4 and MA channels like ELKIN1.

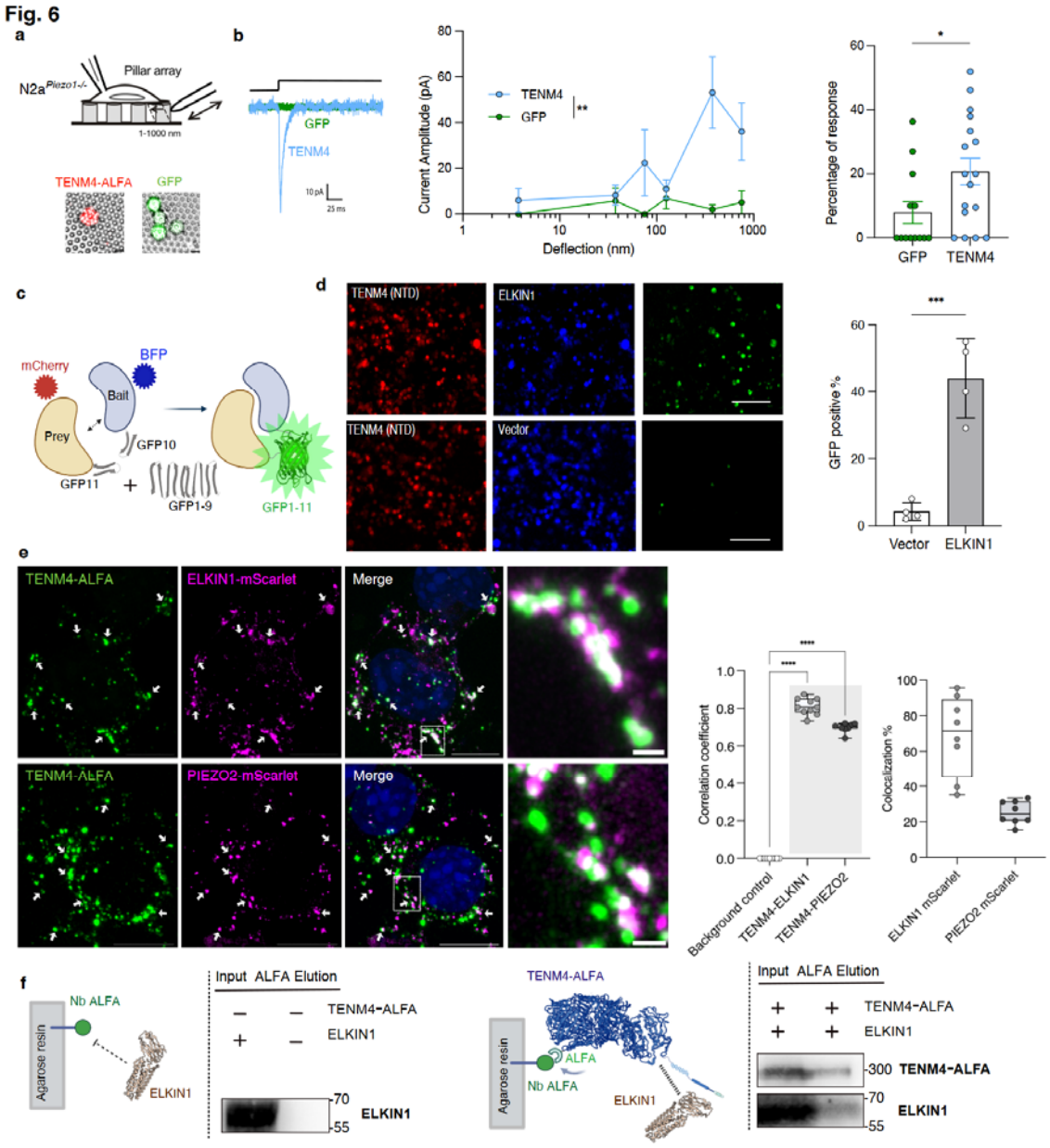

Figure 6

TENM4 interactions with ELKIN1 and PIEZO2. a. Cartoon of pillar stimulation. Example of transfected N2a$^{Piezo1-/-}$ cells expressing Tenm4-ALFA (red) and pRK8-eGFP (green) on pillar array Scale bar 5 µm. **b.** Representative pillar stimulation with current traces evoked from single pilus movements in N2a$^{Piezo1-/-}$ cells expressing Tenm4-ALFA (blue) compared to control pRK8-eGFP

transfected cells (green). Deflection-current amplitude plot showing large increase in the amplitude and sensitivity of MA-currents in cells transfected with TENM4 (blue) compared to control (green). Statistical significance calculated with Kruskal-Wallis test. Right shows that MA-currents were evoked at much higher frequencies, 20.7± 4.2 % in Tenm4-ALFA expressing cells, compared to controls,7.9 ± 3.4%. Statistical significance calculated with Mann-Whitney test. **c**. Schematic of the tripartite split-GFP complementation assay. **d**. HEK293T cells were transfected with three plasmids encoding bait (e.g., ELKIN1)::GFP10, prey (e.g., TENM4)::GFP11 and GFP domain 1-9 proteins. Protein interaction produces complementation and reconstituted GFP fluorescence (green). Representative images showing complementation signals in cells expressing the N-terminal domain (NTD) of TENM4 showing a specific interaction with ELKIN1, not seen in the empty vector control (left 6 panels). Quantification (right) shows a strong interaction between TENM4(NTD) and ELKIN1 Scale bar 100 μm. Statistical analysis with one-way ANOVA followed by Dunnett's multiple comparison test. **e.** Representative super-resolution images of N2a cells co-transfected with a Tenm4-ALFA expression plasmid with mScarlet-ELKIN1 (purple in middle) or PIEZO2-mScarlet (purple in below), arrows indicate co-localization signals. Right higher magnification of co-localized protein region (from white dash boxes) Scale bar is 10μm for cells, 1μm magnified region. Quantification was carried out and a co-localization correlation, ranging from -1 to 1, signifies the strength of overlap. Values near 1 indicate strong co-localization, near -1 indicate separation. TENM4-ELKIN1 and TENM4-PIEZO2 display strong co-localization. Right, TENM4 shows 75% overlap with ELKIN1 and 30% with PIEZO2 on the cell surface. **f.** Co-elution of TENM4-ALFA and ELKIN1 using an ALFA selector resins. Western blot of ALFA pull-down elution from HEK293T cell transfected with TENM4-ALFA and ELKIN1 (right panel) or ALFA vector plasmid and ELKIN1 (left panel). * indicates $p < 0.05$; ** indicates $p < 0.01$; *** indicates $p < 0.001$ means ± s.e.m.

Discussion

Here we show that TENM4 is an essential transduction component for both touch and fast mechanical pain. We also show that sensory neuron expression of TENM4 is required for mechanoreceptor function. We established a novel technology termed PreScission Protein Disassembly which relies on the use of a highly specific protease to acutely manipulate proteins in vivo (see also[51]) . We show that incomplete proteolytic cleavage of TENM4 molecules at the site of transduction is sufficient to completely abolish mechanoreceptor function within minutes (Fig. 3). After PreScission cleavage of TENM4, it took 72 hours for newly synthesized TENM4 to restore both mechanoreceptor function and normal touch evoked behavior. We were surprised at the profound and prolonged disappearance of TENM4 immunoreactivity at sensory endings and assume that cleavage led to clearance of these damaged TENM4 containing complexes that take some time to reassemble. Nevertheless, this

observation clearly demonstrates that the presence of intact TENM4 at the sensory ending is both necessary and sufficient for mechanoreceptor function (Fig. 5). Our data indicate that essentially all sensory neurons with myelinated axons require TENM4 for function, including mechanoreceptors necessary for touch sensation[3,15,19] and Aδ-mechanonociceptors necessary for fast pain[1]. The loss of sensory neuron mechanosensitivity after genetic ablation or proteolytic cleavage of TENM4 was associated with loss of mechanosensitive ion channel function (Fig. 2, 3). Consistently, we show that TENM4 can associate with the mechanically activated ion channels PIEZO2 and ELKIN1, which together can account for most mechanotransduction in myelinated sensory neurons[3,5,20]. We observed little or no effect of TENM4 ablation on C-fiber nociceptors. These findings are consistent with previous results indicating that neither protease sensitive tethers, nor PIEZO2 or ELKIN1 are necessary for C-fiber nociceptor mechanosensitivity[3,5,7,20]. Together our data strongly support a model whereby TENM4 forms part of an essential link between mechanosensitive channels and the extracellular matrix at the neuro-glial endings where transduction takes place. Teneurins play essential roles in nervous system development, in particular during neuronal migration, myelination by oligodendrocytes and synaptogenesis[35,52]. Our data provide an unexpected and surprising link between these proteins and fast mechanotransduction, as we show that the integrity of TENM4 is absolutely necessary for almost all somatic sensation. Indeed the mechanisms by which Teneurins coordinate neurodevelopmental events may well include interactions with mechanosensitive ion channels the roles of which in development have only just started to be investigated[53]. *TENM4* is a risk gene for schizophrenia and bipolar disorder[54,55] thus raising the intriguing possibility that it is a molecular link to sensory disturbances found in such patients[56]. The fact that TENM4 protein integrity is necessary for normal touch and pain sensation makes this protein a new and desirable target for novel analgesic therapy.

References

1. Arcourt A, Gorham L, Dhandapani R, et al. Touch Receptor-Derived Sensory Information Alleviates Acute Pain Signaling and Fine-Tunes Nociceptive Reflex Coordination. *Neuron*. 2017;93(1):179-193. doi:10.1016/j.neuron.2016.11.027

2. Lewin GR, Moshourab R. Mechanosensation and pain. *J Neurobiol*. 2004;61(1):30-44. doi:10.1002/neu.20078

3. Ranade SS, Woo SH, Dubin AE, et al. Piezo2 is the major transducer of mechanical forces for touch sensation in mice. *Nature*. 2014;516(7529):121-U330. doi:10.1038/nature13980

4. Poole K, Herget R, Lapatsina L, Ngo HD, Lewin GR. Tuning Piezo ion channels to detect molecular-scale movements relevant for fine touch. *Nat Commun*. 2014;5:3520. doi:10.1038/ncomms4520

5. Chakrabarti S, Klich JD, Khallaf MA, et al. Touch sensation requires the mechanically gated ion channel ELKIN1. *Science*. 2024;383(6686):992-998. doi:10.1126/science.adl0495

6. Patkunarajah A, Stear JH, Moroni M, et al. TMEM87a/Elkin1, a component of a novel mechanoelectrical transduction pathway, modulates melanoma adhesion and migration. *Elife*. 2020;9. doi:10.7554/eLife.53308

7. Hu J, Chiang LY, Koch M, Lewin GR. Evidence for a protein tether involved in somatic touch. *Embo J*. 2010;29(4):855-867. doi:10.1038/emboj.2009.398

8. Jin P, Jan LY, Jan YN. Mechanosensitive Ion Channels: Structural Features Relevant to Mechanotransduction Mechanisms. *Annu Rev Neurosci Vol 36*. 2020;43:207-229. doi:10.1146/annurev-neuro-070918-050509

9. Cox CD, Bavi N, Martinac B. Bacterial Mechanosensors. *Annu Rev Physiol*. 2018;80(1):71-93. doi:10.1146/annurev-physiol-021317-121351

10. Qiu X, Müller U. Sensing sound: Cellular specializations and molecular force sensors. *Neuron*. 2022;110(22):3667-3687. doi:10.1016/j.neuron.2022.09.018

11. Chung YD, Zhu J, Han Y, Kernan MJ. nompA encodes a PNS-specific, ZP domain protein required to connect mechanosensory dendrites to sensory structures. *Neuron*. 2001;29(2):415-428.

12. Göpfert MC, Humphris ADL, Albert JT, Robert D, Hendrich O. Power gain exhibited by motile mechanosensory neurons in Drosophila ears. *Proc Natl Acad Sci U S A*. 2005;102(2):325-330. doi:10.1073/pnas.0405741102

13. Goodman MB, Sengupta P. How Caenorhabditis elegans Senses Mechanical Stress, Temperature, and Other Physical Stimuli. *Genetics*. 2019;212(1):25-51. doi:10.1534/genetics.118.300241

14. Abraira VE, Ginty DD. The sensory neurons of touch. *Neuron*. 2013;79(4):618-639. doi:10.1016/j.neuron.2013.07.051

15. Ojeda-Alonso J, Calvo-Enrique L, Paricio-Montesinos R, et al. Sensory Schwann cells set perceptual thresholds for touch and selectively regulate mechanical nociception. *Nat Commun*. 2024;15(1):898. doi:10.1038/s41467-024-44845-8

16. Schwaller F, Begay V, Garcia-Garcia G, et al. USH2A is a Meissner's corpuscle protein necessary for normal vibration sensing in mice and humans. *Nat Neurosci.* 2021;24(1):74-81. doi:10.1038/s41593-020-00751-y

17. Abdo H, Calvo-Enrique L, Lopez JM, et al. Specialized cutaneous Schwann cells initiate pain sensation. *Science*. 2019;365(6454):695-699. doi:10.1126/science.aax6452

18. Wetzel C, Pifferi S, Picci C, et al. Small-molecule inhibition of STOML3 oligomerization reverses pathological mechanical hypersensitivity. *Nat Neurosci.* 2017;20(2):209-218. doi:10.1038/nn.4454

19. Wetzel C, Hu J, Riethmacher D, et al. A stomatin-domain protein essential for touch sensation in the mouse. *Nature*. 2007;445(7124):206-209. doi:10.1038/nature05394

20. Murthy SE, Loud MC, Daou I, et al. The mechanosensitive ion channel Piezo2 mediates sensitivity to mechanical pain in mice. *Sci Transl Med.* 2018;10(462):eaat9897. doi:10.1126/scitranslmed.aat9897

21. Poole CB, Jin J, McReynolds LA. Cloning and biochemical characterization of blisterase, a subtilisin-like convertase from the filarial parasite, Onchocerca volvulus. *J Biol Chem*. 2003;278(38):36183-36190. doi:10.1074/jbc.M302601200

22. Sherman BT, Hao M, Qiu J, et al. DAVID: a web server for functional enrichment analysis and functional annotation of gene lists (2021 update). *Nucleic Acids Res*. 2022;50(W1):W216-W221. doi:10.1093/nar/gkac194

23. Huang DW, Sherman BT, Lempicki RA. Systematic and integrative analysis of large gene lists using DAVID bioinformatics resources. *Nat Protoc*. 2009;4(1):44-57. doi:10.1038/nprot.2008.211

24. Visel A, Thaller C, Eichele G. GenePaint.org: an atlas of gene expression patterns in the mouse embryo. *Nucleic Acids Res*. 2004;32(Database issue):D552-6. doi:10.1093/nar/gkh029

25. McCarter GC, Reichling DB, Levine JD. Mechanical transduction by rat dorsal root ganglion neurons in vitro. *Neurosci Lett*. 1999;273(3):179-182. doi:10.1016/s0304-3940(99)00665-5

26. Chiang LY, Poole K, Oliveira BE, et al. Laminin-332 coordinates mechanotransduction and growth cone bifurcation in sensory neurons. *Nat Neurosci.* 2011;14(8):993-1000. doi:10.1038/nn.2873

620 27. Pavlakis E, Chiotaki R, Chalepakis G. The role of Fras1/Frem proteins in the structure and function of basement membrane. *Int J Biochem Cell Biol*. 2011;43(4):487-495. doi:10.1016/j.biocel.2010.12.016

28. Nakamura H, Cook RN, Justice MJ. Mouse Tenm4 is required for mesoderm induction. *BMC Dev Biol*. 2013;13:9. doi:10.1186/1471-213X-13-9

625 29. Chakrabarti S, Pattison LA, Doleschall B, et al. Intraarticular Adeno-Associated Virus Serotype AAV-PHP.S-Mediated Chemogenetic Targeting of Knee-Innervating Dorsal Root Ganglion Neurons Alleviates Inflammatory Pain in Mice. *Arthritis Rheumatol Hoboken NJ*. 2020;72(10):1749-1758. doi:10.1002/art.41314

30. Chan KY, Jang MJ, Yoo BB, et al. Engineered AAVs for efficient noninvasive gene delivery
630 to the central and peripheral nervous systems. *Nat Neurosci*. 2017;20(8):1172-1179. doi:10.1038/nn.4593

31. Mosca TJ. On the Teneurin track: a new synaptic organization molecule emerges. *Front Cell Neurosci*. 2015;9:204. doi:10.3389/fncel.2015.00204

32. Mosca TJ, Hong W, Dani VS, Favaloro V, Luo L. Trans-synaptic Teneurin signalling in
635 neuromuscular synapse organization and target choice. *Nature*. 2012;484(7393):237-241. doi:10.1038/nature10923

33. Feng K, Zhou XH, Oohashi T, et al. All four members of the Ten-m/Odz family of transmembrane proteins form dimers. *J Biol Chem*. 2002;277(29):26128-26135. doi:10.1074/jbc.M203722200

640 34. Tucker RP, Chiquet-Ehrismann R. Teneurins: a conserved family of transmembrane proteins involved in intercellular signaling during development. *Dev Biol*. 2006;290(2):237-245. doi:10.1016/j.ydbio.2005.11.038

35. Del Toro D, Carrasquero-Ordaz MA, Chu A, et al. Structural Basis of Teneurin-Latrophilin Interaction in Repulsive Guidance of Migrating Neurons. *Cell*. 2020;180(2):323-339.e19.
645 doi:10.1016/j.cell.2019.12.014

36. Li L, Ginty DD. The structure and organization of lanceolate mechanosensory complexes at mouse hair follicles. *eLife*. 2014;3:e01901.

37. Walcher J, Ojeda-Alonso J, Haseleu J, et al. Specialized mechanoreceptor systems in rodent glabrous skin. *J Physiol*. 2018;596(20):4995-5016. doi:10.1113/JP276608

650 38. Stucky CL, Lewin GR. Isolectin B(4)-positive and -negative nociceptors are functionally distinct. *J Neurosci*. 1999;19(15):6497-6505.

39. Heidenreich M, Lechner SG, Vardanyan V, et al. KCNQ4 K(+) channels tune mechanoreceptors for normal touch sensation in mouse and man. *Nat Neurosci*. 2012;15(1):138-145. doi:10.1038/nn.2985

40. Hu J, Lewin GR. Mechanosensitive currents in the neurites of cultured mouse sensory neurones. *J Physiol*. 2006;577(Pt 3):815-828. doi:10.1113/jphysiol.2006.117648

41. Kress M, Koltzenburg M, Reeh PW, Handwerker HO. Responsiveness and functional attributes of electrically localized terminals of cutaneous C-fibers in vivo and in vitro. *J Neurophysiol*. 1992;68(2):581-595. doi:10.1152/jn.1992.68.2.581

42. Koltzenburg M, Stucky CL, Lewin GR. Receptive properties of mouse sensory neurons innervating hairy skin. *J Neurophysiol*. 1997;78(4):1841-1850. doi:10.1152/jn.1997.78.4.1841

43. Kumar P, Aradhyam GK. Easy and efficient protocol for purification of recombinant peptides. *Protein Expr Purif*. 2014;95:129-135. doi:10.1016/j.pep.2013.12.004

44. Lossie AC, Nakamura H, Thomas SE, Justice MJ. Mutation of l7Rn3 shows that Odz4 is required for mouse gastrulation. *Genetics*. 2005;169(1):285-299. doi:10.1534/genetics.104.034967

45. Götzke H, Kilisch M, Martínez-Carranza M, et al. The ALFA-tag is a highly versatile tool for nanobody-based bioscience applications. *Nat Commun*. 2019;10(1):4403. doi:10.1038/s41467-019-12301-7

46. Ojeda-Alonso J, Begay V, Garcia-Contreras JA, Campos-Perez AF, Purfurst B, Lewin GR. Lack of evidence for participation of TMEM150C in sensory mechanotransduction. *J Gen Physiol*. 2022;154(12). doi:10.1085/jgp.202213098

47. Moroni M, Servin-Vences MR, Fleischer R, Sánchez-Carranza O, Lewin GR. Voltage gating of mechanosensitive PIEZO channels. *Nat Commun*. 2018;9(1):1096. doi:10.1038/s41467-018-03502-7

48. Li J, Bandekar SJ, Arac D. The structure of fly Teneurin-m reveals an asymmetric self-assembly that allows expansion into zippers. *Embo Rep*. 2023;24(6):e56728. doi:10.15252/embr.202256728

49. Wu X, Hammer JA. ZEISS Airyscan: Optimizing Usage for Fast, Gentle, Super-Resolution Imaging. *Methods Mol Biol Clifton NJ*. 2021;2304:111-130. doi:10.1007/978-1-0716-1402-0_5

50. Verkest C, Schaefer I, Nees TA, et al. Intrinsically disordered intracellular domains control key features of the mechanically-gated ion channel PIEZO2. *Nat Commun*. 2022;13(1):1365. doi:10.1038/s41467-022-28974-6

51. Sanfeliu-Cerdán N, Català-Castro F, Mateos B, et al. A MEC-2/stomatin condensate liquid-to-solid phase transition controls neuronal mechanotransduction during touch sensing. *Nat Cell Biol*. 2023;25(11):1590-1599. doi:10.1038/s41556-023-01247-0

52. Hor H, Francescatto L, Bartesaghi L, et al. Missense mutations in TENM4, a regulator of axon guidance and central myelination, cause essential tremor. *Hum Mol Genet*. 2015;24(20):5677-5686. doi:10.1093/hmg/ddv281

53. Pillai EK, Franze K. Mechanics in the nervous system: From development to disease. *Neuron*. 2024;112(3):342-361. doi:10.1016/j.neuron.2023.10.005

54. Ikeda M, Takahashi A, Kamatani Y, et al. A genome-wide association study identifies two novel susceptibility loci and trans population polygenicity associated with bipolar disorder. *Mol Psychiatry*. 2018;23(3):639-647. doi:10.1038/mp.2016.259

55. Xue CB, Xu ZH, Zhu J, et al. Exome Sequencing Identifies TENM4 as a Novel Candidate Gene for Schizophrenia in the SCZD2 Locus at 11q14-21. *Front Genet*. 2018;9:725. doi:10.3389/fgene.2018.00725

56. Dworkin RH. Pain insensitivity in schizophrenia: a neglected phenomenon and some implications. *Schizophr Bull*. 1994;20(2):235-248. doi:10.1093/schbul/20.2.235

57. Aricescu AR, Lu W, Jones EY. A time- and cost-efficient system for high-level protein production in mammalian cells. *Acta Crystallogr D Biol Crystallogr*. 2006;62(Pt 10):1243-1250. doi:10.1107/S0907444906029799

58. Rocio Servin-Vences M, Moroni M, Lewin GR, Poole K. Direct measurement of TRPV4 and PIEZO1 activity reveals multiple mechanotransduction pathways in chondrocytes. Swartz KJ, ed. *eLife*. 2017;6:e21074. doi:10.7554/eLife.21074

59. Chaplan SR, Bach FW, Pogrel JW, Chung JM, Yaksh TL. Quantitative assessment of tactile allodynia in the rat paw. *J Neurosci Methods*. 1994;53(1):55-63. doi:10.1016/0165-0270(94)90144-9

60. Gonzalez-Cano R, Boivin B, Bullock D, Cornelissen L, Andrews N, Costigan M. Up-Down Reader: An Open Source Program for Efficiently Processing 50% von Frey Thresholds. *Front Pharmacol*. 2018;9:433. doi:10.3389/fphar.2018.00433

61. Cabantous S, Nguyen HB, Pedelacq JD, et al. A new protein-protein interaction sensor based on tripartite split-GFP association. *Sci Rep*. 2013;3:2854. doi:10.1038/srep02854

62. Hughes CS, Foehr S, Garfield DA, Furlong EE, Steinmetz LM, Krijgsveld J. Ultrasensitive proteome analysis using paramagnetic bead technology. *Mol Syst Biol*. 2014;10(10):757. doi:10.15252/msb.20145625

63. Demichev V, Messner CB, Vernardis SI, Lilley KS, Ralser M. DIA-NN: neural networks and interference correction enable deep proteome coverage in high throughput. *Nat Methods*. 2020;17(1):41-44. doi:10.1038/s41592-019-0638-x

64. Ritchie ME, Phipson B, Wu D, et al. limma powers differential expression analyses for RNA-sequencing and microarray studies. *Nucleic Acids Res*. 2015;43(7):e47. doi:10.1093/nar/gkv007

65. Perez-Riverol Y, Bai J, Bandla C, et al. The PRIDE database resources in 2022: a hub for mass spectrometry-based proteomics evidences. *Nucleic Acids Res*. 2022;50(D1):D543-D552. doi:10.1093/nar/gkab1038

730

Methods

Animals

All experiments were approved by the Berlin Animal Ethics Committees (Landesamt für Gesundheit und Soziales) and carried out in accordance with European animal welfare law. Wild-type (C57BL/6N) adult (8-30 weeks) mice of both sexes were used. Mice were housed in groups of 5 with food, water and enrichment available ad libitum.

The *Tenm4*$^{KI/+}$ mouse line was generated by the Ingenious Targeting Laboratory (Ronkonkoma, NY) using homologous recombination in mouse ES cells. Targeted iTL IN2 (C57BL/6) embryonic stem cells were microinjected into Balb/c blastocysts. Resulting chimeras with a high percentage black coat color were mated to C57BL/6 FLP mice to generate Somatic Neo Deleted mice. This involved the replacement of the amino acids HLYTQSL (exon 27) with the PreScission Protease target sequence LEVLFQG, as illustrated in Extended Data Fig. 1. After the removal of the Neo cassette, a single FRT site of 78 bp is retained and subsequently utilized for the selection process and genotyping. The genotyping strategy utilized was as follows: Forward primer: 5'- GGGAAATGGGATGGTGGGAA -3', reverse primer: 5'- ACCCACGTGGAGTTGTTCTTC -3'. The expected band for WT is 231 bp, while for *Tenm4*$^{PreS.\ KI/+}$, two bands are observed at 231 and 309 bp.

Frem2$^{fl/fl}$ and *Tenm4*$^{fl/fl}$ mouse lines were generated at Shanghai Model Organisms Center using the CRISPR/Cas9 strategy. *Frem2*$^{fl/fl}$ *and Tenm4*$^{fl/fl}$ mice, carring LoxP sites flanking exon 12 and exon 7, respectively, were generated using the following gRNAs *Frem2*$^{fl/fl}$-gRNA1 (5'- ACAAGACTAGCTCTGGGTCTGGG -3'), *Frem2*$^{fl/fl}$-gRNA2 (5'-TACAGAGATAACAGTGGGGGTGG -3'), *Tenm4*$^{fl/fl}$-gRNA1 (5'-AGAGCCCAGTCTCTCACCAGTGG -3') and *Tenm4*$^{fl/fl}$-gRNA2 (5'-GCACTGAACCTCAGCCCTGGTGG -3'). The *Frem2*$^{fl/fl}$ genotyping strategy utilized was

as follows: forward primer (5'- AGTCGGGTTTCTTCTTCCACAA -3'), reverse primer (5'-CCCAAAAGGTCACATGCTAATCTAT -3'). The expected band for WT is 197 bp, while for *Frem2*$^{f/fl}$, a band with 263 bp. The *Tenm4*$^{fl/fl}$ genotyping strategy utilized was as follows: forward primer (5'- TGAACCATGCATCCCTCACC -3'), reverse primer (5'-AAACTCCCACCCCACTGAAC -3'). The expected band for WT is 313 bp, while for *Tenm4*$^{fl/fl}$, a band with 379 bp. Animals of various genotypes were randomly selected for experiments based on their availability.

AAV transduction

pAAV-Syn-Cre-p2A-EGFP (4.91 x 10^{12} vg/ml) and *pAAV-hSyn-NLS-GFP-P2A* (4.98 x 10^{12} vg/ml) were manufactured in the Charité Viral Core facility (Berlin, Germany). *Frem2*^{CKO} and *Tenm4*^{CKO} were generated by retroorbital injection of Adeno-associated virus (*pAAV-Syn-Cre-p2A-eGFP*) in *Frem2*$^{fl/fl}$ and *Tenm4*$^{fl/fl}$, respectively, to induce Cre/GFP recombinase expression in DRG neurons. Subsequently, DNA between the LoxP sites will be excised, leading to a frameshift mutation and the production of a truncated protein as illustrated in Extended Data Fig 1. Control mice were generated by similar injections of *pAAV-hSyn-NLS-GFP-P2A* that induce GFP expression in DRG neurons. Afterwards the animals were returned to their home cage for at least three weeks to achieve a adequate recombination and subsequently tested in electrophysiological and behavioral assays.

Tamoxifen injections

Tamoxifen-induced activation of Cre recombinase under the Advillin promoter in sensory neurons was used as a second inducible approach to delete *Tenm4* using the Advillin-CreERT2 transgenic mice (*Tenm4*$^{fl/fl}$*; Avil*$^{CreERT2/WT}$). Briefly, *Tenm4*$^{fl/fl}$*; Avil*$^{CreERT2/WT}$ mice were injected intraperitoneally with corn oil (control animals) or Tamoxifen (15mg/ml) solubilized in corn oil (Sigma) for 5 consecutive days. Prior to injection, each mouse was

weighed to ensure the administration of a uniform tamoxifen dose (150 mg/kg). Behavioral assays were performed 21 days after vehicle or tamoxifen injections

PreScission injections and *ex vivo* cleavage assay

Adult mice (8-30 weeks old) were anesthetized using a 5% isoflurane-air mixture in a transparent box, with anesthesia maintenance via a 2.5% isoflurane-air mixture through a plastic tube. After achieving slow, steady breathing, a hind paw pinch test assessed pain reflexes. Subsequently, mice received a 10μL injection of saline NaCl solution (control group) or a 20% diluted PreScission protease in saline NaCl solution (v/v) 10 U/μL, Cytiva, Lot: 18043250). The injection was directed into the intraplanar surface of glabrous skin or the top of the hairy skin of the hind paw. The mice were then used for for immunohistochemistry, electrophysiological, or behavioral experiments.

For *ex vivo* PreScission protein cleavage assay,*Tenm4*$^{KI/+}$and WT mice were administered injections of 20% PreScission protease (2-10 U/μL, Cytiva, Lot: 18043250) diluted in NaCl (v/v) in the glabrous skin of hind paws. Tissues were collected one-hour post-injection for protein extraction. Frozen tissues (-80°C) were powdered using a mortar and added to lysis buffer (RIPA) containing 50 mM Tris pH 7.5, 150 mM NaCl, 0.1% SDS, 1.0% NP-40, 0.5% deoxycholate, and a protease inhibitor cocktail tablet. Sonication (magnitude 3) with 10 seconds on and 50 seconds off was applied three times to each sample. The lysate was centrifuged at 13,200xg for 30 minutes. Samples corresponding to 1/100 of the input were resolved by SDS–PAGE. Analysis was conducted by Western blotting using a polyclonal sheep-raised antibody against TENM4 (dilution 1:500), followed by an HRP-conjugated goat anti-sheep IgG (R&D Lot: 1522051, dilution 1:10,000). Blots were developed using the SuperSignal™ West Dura ECL Kit (Thermo Scientific) and imaged using a Bio-Rad ChemiDoc™ MP imaging system.

Plasmids and cloning

Teneurins 1-4 and Elkin1 were independently cloned into modified plasmids, incorporating the BsmBI restriction site as detailed in the tripartite-GFP method section. This involved using specific primers for each construct: TENM1 (1-526): forward primer (5'-cacgtctcactccatggagcaaacagactgcaaa -3'), reverse primer (5'-cacgtctcacttattcaattgctgtagttagcacaaat-3'), TENM2 (1-571): forward primer (5'-cacgtctcacttattcaattgctgtagttagcacaaat -3'), reverse primer (5'-ggatctgaattcttaatctaagacaacagtgttgaaggag -3'), TENM3 (1-513): forward primer (5'-cacgtctcactccatggatgtgaaggaacgcag -3'), reverse primer (5'-cacgtctcacttactctataacgatcgtgttaaaggagac -3'), TENM4 (1-561): forward primer (5'-cacgtctcactccatggagccagaccactcg -3'), reverse primer (5'-cacgtctcacttaatccagatactggatgaaaccgg -3'), and Elkin1 (full length): forward primer (5'-cacgtctcacaccatggcggtggctgc -3'), reverse primer (5'- cacgtctcatcccctccatctttgacctttcaaagtg -3') (Clontech). The full-length Tenm4 cDNA, sourced from VectorBuilder.inc (Mouse MGC Verified FL clone, ID: NM_011858.4, VB221104-1135), containing a modified C-terminus ALFA tag. Additionally, the full-length PIEZO2 cDNA with an mScarlet red fluorescent protein tag plasmid was obtained as a gift from Professor Stefan Lechner at UKE Hamburg. Furthermore, the recently-published full-length ELKIN1 pRK8-eGFP[6], was adapted to incorporate mScarlet at the N-terminus using specific primers forward primer (5'-ctatcgattgaattaagcttatggtgagcaagggcgag -3'), reverse primer (5'-caccgccatggtggcggatcccttgtacagctcgtccatgcc -3') (Clontech).

Cell line culture:

HEK293T cells were cultured in DMEM-Glutamax (Gibco, ThermoFisher Scientific) supplemented with 10% fetal bovine serum (FBS, PAN Biotech GmbH) and 1% penicillin and streptomycin (P/S, Sigma-Aldrich). N2a cells were cultured in DMEM-Glutamax (Gibco, ThermoFisher Scientific) supplemented with 45% Opti-MEM (Gibco, ThermoFisher Scientific), 10% FBS, and 1% penicillin and streptomycin (P/S, Sigma-Aldrich). For downstream analyses, HEK293T and N2a cells were transiently transfected by plating them on glass coverslips coated with poly-L-lysine and laminin at various cell densities and maintained overnight in a 37°C, 5% CO2 incubator. Transfections were carried out using 4µL FuGene HD per 50µL of Opti-MEM with 1µg of cDNA, following the manufacturer's instructions. Subsequent analyses were performed 48 hours post-transfection, and data were derived from a minimum of 3 independent transfections.

Immunocytochemistry:

Cells were fixed in 4% paraformaldehyde in PBS for 10 minutes at room temperature, followed by three washes with PBS. Subsequently, cells were blocked for 1 hour with 10% horse serum in PBS, either in the presence or absence of 0.1% (v/v) Triton X-100 for staining intracellular or extracellular epitopes, respectively. Following blocking, cells were incubated overnight at 4°C with primary antibodies, appropriately diluted in either 3% horse serum in PBS or 3% horse serum in 0.1% (v/v) Triton X-100/PBS, depending on the location of the epitope, for epifluorescence staining or cellular staining, respectively. Primary antibodies included polyclonal sheep anti-TENM4 antibody at a dilution of 1:500 (R&D Systems (TENM4-N), Catalog #: AF6320), our own polyclonal rabbit anti-TENM4 antibody at a dilution of 1:1000 (TENM4-C) (Eurogentec), and FluoTag®-X2 anti-ALFA at a dilution of 1:500 (NanoTag, N1502-Ab635P-L). When FluoTag®-X2 anti-ALFA was employed for Alfa-tagged protein detection, the incubation time was reduced to 1.5 hours at room temperature. Following three washes with PBS, cells were incubated for 1.5 hours at room

temperature with species-specific conjugated secondary antibodies diluted at 1:500 in PBS: Donkey anti-Sheep IgG (H+L) Cross-Adsorbed Secondary Antibody, Alexa Fluor™ 568 (Invitrogen, Catalog # A-21099), and goat anti-Rabbit IgG (H+L) Cross-Adsorbed Secondary Antibody, Alexa Fluor™ 555 (Invitrogen, Catalog # A-21428). This step was omitted when using FluoTag®-X2 anti-ALFA. After three washes in PBS, cells were stained with DAPI diluted 1:1000 in PBS for 10 minutes at room temperature, followed by three additional washes in PBS, and finally, mounting with Dako (Agilent, S3023).

Multiplex fluorescent *in situ* hybridization

Tenm4, *Kcnq4*, *Elkin1* and *Piezo2* mRNA levels were assessed in DRGs from WT (n = 4) mice using RNAscope Multiplex Fluorescent Kit v2 (a fluorescent *in situ* hybridization technology). Briefly, the 12µm DRG sections were immersed in PBS for 15 minutes and dehydrated in a series of 50 %, 70 %, 100 % ethanol for 5 minutes each. Afterwards, sections were treated with a hydrogen peroxide solution for 15 minutes at room temperature to block endogenous peroxidase activity followed by another wash with 100% ethanol for 5 minutes. Next, Protease plus was applied for 30 minutes at RT. After three washes with PBS, probes were applied, and hybridization was carried out in a humified oven at 40°C for 2h. Following hybridization, amplification was performed using Amp1, Amp2, and Amp3 each for 30 minutes at 40°C. For detection, each section was treated sequentially with channel specific HRP (HRP-C1, HRP-C1, HRP-C3) for 15 minutes, followed by TSA-mediated fluorophore binding for 30 minutes and final HRP blocking for 15 minutes (all steps at 40°C). The following probes were used: *Tenm4*- Mm-*Tenm4* (C1 #555491), *Kcnq4*- Mm-*Kcnq4* (C2 #472271), *Piezo2* - Mm-*Piezo2*-E43-E45 15 (C1 #439971) and *Elkin1* - Mm-*Tmem87a* (C3 #868581). The fluorophores applied to detect the signal from the probes were Opal 690 Reagent (1:750; Akoya Biosciences, #FP1497001KT) or Opal 570 Reagent (1:750; Akoya Biosciences, #FP1488001KT). Slides were rinsed with PBS-tween, followed by a 1-hour

incubation at room temperature in an antibody diluent solution. Following this, they were treated for antibody immunostaining according to procedures outlined below. Lastly, the slides were exposed to RNAscope DAPI during the final incubation. Images were obtained using Airyscan fluorescence microscope (Axio, Zeiss). Exposure levels were kept constant for each slide and the same contrast enhancements were made to all slides. In the quantification experiments, over 700 neurons were counted in each group, with a representation of 2 male and 3 female mice in each group.

Generation of anti TENM4 antibody (Anti-TENM4-C)

The antigen used for the generation of this polyclonal antibody consisted of most of the extracellular domain of murine TENM4 (UniProt ID Q3UHK6), including the large YD shell. The expression construct for the production of the antigen was synthesized by VectorBuilder GmbH (pRP[Exp]-CMV) and comprised amino acids 921 to 2771, resulting in secretion[57] (µ-phosphatase secretion leader sequence MGILPSPGMPALLSLVSLLSVLLMGCVA*ETG) of a C-terminal His6-tagged protein. The protein was produced in ExpiCHO-S™ cells (Thermo Fisher Scientific) at 31°C and 8% CO2 using BalanCD transfectory CHO medium (FUJIFILM Irvine Scientific) supplemented with 4 mM GlutaMAX (Thermo Fisher Scientific). Cells were transiently transfected using PEI MAX (Polysciences) and supplemented with 6 g/L glucose (Sigma) three days after transfection. Cell culture supernatant was collected six days after transfection, filtered through 0.22 µm filters, and supplemented with 0.5 M NaCl, 5 mM imidazole, and 25 mM sodium phosphate buffer pH 7.8. The protein was captured from the supernatant by affinity chromatography using cOmplete™ His-Tag Purification Resin (Roche), equilibrated with 50 mM sodium phosphate pH 7.8, 0.5 M NaCl, and 5 mM imidazole. The bound protein was first washed with 50 mM sodium phosphate pH 7.8, 0.5 M NaCl, followed by a buffer containing 10 mM imidazole to remove contaminating proteins. The protein was eluted with the same buffer containing 0.25

M imidazole. The protein was further purified by gel filtration on a 16/60 HiPrep Sephacryl S-400 HR column (Cytiva) equilibrated with PBS buffer pH 7.4 and 0.2 M NaCl. The purified protein was concentrated to about 3 mg/mL, sterile filtered, flash-frozen in small aliquots with liquid nitrogen and stored at -70°C until further use.

The purified antigen was then used by Eurogentec for immunization of rabbits. Two animals were injected 4 times with 100 µg of antigen. The final bleed was collected 28 days after the first injection and subsequently concentrated using affinity purification.

Immunohistochemistry

Mice were euthanized by cervical dislocation, and tissues including hairy and glabrous skin, sciatic nerves, and DRGs, were collected. The hairy skins were shaved, and the hypodermis, ligaments, and attached muscle tissue were removed from the skin samples. Subsequently, skin samples were stretched out using insect pins and fixed in 4% paraformaldehyde (PFA) for a duration of 4 hours then post-fixed at 4 °C for 24 h in 20% dimethylsulfoxide and 80% methanol, while sciatic nerve and DRG samples were fixed in 4% PFA for a duration of 2 hours. L2–L5 DRG and sciatic nerves were dissected and postfixed in PFA for 1 hour. Samples underwent cryoprotection with an overnight incubation in 30% (w/v) sucrose solution in 5% PBS at 4°C, followed by embedding in optimal cutting temperature compound (OCT compound; Thermo Fisher Scientific).

Abdominal human skin samples were obtained from patients that underwent plastic surgery (written consent obtained, ethics approval from Charité University Hospital EA1/356/21). Following surgical removal, excessive subcutaneous fat tissue was removed and skin sheets were either directly used or stored at -20°C until further usage.

OCT-embedded samples were snap-frozen on dry ice and stored at −80 °C. Sciatic nerve- and DRGs- embedded tissues were sectioned at 12µm using a Leica Cryostat (CM3000;

925 Nussloch), mounted on Superfrost-Plus microscope slides (Thermo Fisher Scientific) and stored at −80 °C until staining. Skin-embedded tissues were sectioned at 60μm and stored in freezing solution (30% (v:v) glycerol, 30% ethylene glycol, and 40% PBS). During staining, slides and free-floating skin sections were washed with PBS-tween and blocked in antibody diluent solution containing 0.2% (v/v) Triton X-100, 5% (v/v) horse serum, and 1% (v/v)
930 bovine serum albumin in PBS for 1 hour at room temperature. Subsequently, slides underwent a 12-hour incubation, while skin samples were incubated for 72 hours at 4°C with primary antibodies. The following primary antibodies were used: anti-TENM4 in Fig. 1 and Extended Data Fig. 2 and 3 (host: sheep, AF6320 and ab215052, 1:500), anti-S100 (host: rabbit, 15146-1-AP, 1:1000), anti-NF200 (host: chicken, AB72996, 1:1000), anti-CK20 (host:
935 guinea pig, BP5080, 1:500), anti-cRET (host: rabbit, 18121, 1:100), anti-CGRP (host: rabbit, 24112, 1:500), anti-TH (host: sheep, AB1542, 1:1000), anti-PGP9.5 (host: mouse, ab20559, 1:500), anti-PV (host: rabbit, PV-27, 1:500), anti-TRKC (host: goat, AF1404, 1:1000), anti-Tmem87a (host: rabbit, HPA018104, 1:100), anti-Frem2 (host: rabbit, sc-98471, 1:400), anti-Slit1 (host: rabbit, ab10984, 1:400), anti-Scribble (host: rabbit, ab154067, 1:400), anti-Pcsk5
940 (host: rabbit, TA332044, 1:400), anti-Tecta (host: mouse, ABNOH00007007-A01, 1:100). Slides and free-floating skin sections were then washed three times using PBS-tween and incubated with the following species-specific conjugated secondary antibodies at 1:500 dilution: Alexa Fluor 488 anti-rabbit (A21206), Alexa Fluor 568 anti-sheep (A21099), Alexa Fluor 568 anti-chicken (A11041), Alexa Fluor 555 anti-goat (A21432), Alexa Fluor 568 anti-
945 guinea pig (106-165-003), or Isolectin GS B4 conjugated to Alexa 594 (121413, Thermo Fisher) overnight at 4 °C. The secondary antibody was washed three times in PBS tween, and DRG and sciatic nerve slides mounted with Dako (Agilent, S3023), while skin samples were processed for tissue clearing using 2,2'-thiodiethanol (TDE, Sigma-Aldrich). Skin sections were then placed in increasing concentrations of TDE every 2 h, from 10% to 25%, 50%

and 97%, in which samples were stored and mounted on to slides and cover slipped. Slides and free-floating skin sections and imaged with Airyscan fluorescence microscope (Axio, Zeiss). Exposure levels were kept constant for each slide and the same contrast enhancements were made to all slides. Negative controls without the primary antibody showed no staining with either secondary. In the quantification experiments, over 700 neurons were counted in each group, with a representation of 2 male and 3 female mice in each group.

DRG neuron culture

Lumbar DRGs (L1-L6) were collected from mice into plating medium (DMEM-F12, Gibco, ThermoFisher Scientific) supplemented with 10% fetal horse serum (FHS, Life Technologies) and 1% penicillin and streptomycin (P/S, Sigma-Aldrich). A single-cell suspension was obtained by enzymatic digestion, first in 1.25% Collagenase IV (1 mg/ml, Sigma-Aldrich) for 1 hour at 37°C and then in 2.5% Trypsin (Sigma-Aldrich) for 15 minutes at 37°C, followed by mechanical trituration with a P1000 pipette tip and purification on a 15% fraction V BSA column. Subsequently, neurons were plated on glass-bottomed dishes coated with poly-L-lysine and laminin for indentation assays or immunostaining. The cultured neurons were incubated in a standard incubator (37°C and 5% CO2). Electrophysiological experiments involving indentation were conducted 18-24 hours after plating, while immunostaining experiments were performed 48 hours after plating. For the MA-current analysis of *Tenm4*$^{fl/fl}$ animals, n = 4 mice underwent AAV-GFP injection (control), and n = 5 mice underwent AAV-Cre injection. For the MA-current analysis of the effects of PreScission on WT and *TENM4*$^{PreS.\ KI/+}$ mice, n = 5 WT, and n = 4 *TENM4*$^{PreS.\ KI/+}$ mice were utilized. Sample sizes were determined based on previous studies with similar effect sizes.

Real-time PCR:

Total RNA was extracted from the skin, DRG, and sciatic nerve of WT mice using the ReliaPrep™ RNA Miniprep Systems and retro-transcribed into cDNA using the GoScript™ Reverse Transcriptase kit, according to the manufacturer's instructions. The expression of TENM4 was evaluated using SYBR Green Real-Time PCR (Thermo Fisher Scientific™). The PCR mix contained 2µl of a 1:10 diluted cDNA template; 5µl of 2x SYBR® Green Master Mix (BioRad); 0.3µl of a 10µM forward primer; 0.3µl of a 10µM reverse primer; 0.5µl of DMSO; 1.9µl of H2O, in a total volume of 10µl per sample. The primers used were the forward primer (5' – cccatcagcaactctcaggac -3') and the reverse primer (5'-ccccgaggatagacttgct -3'). Standard reactions were carried out using a CFX Connect Real-Time PCR Detection System. Technical triplicates were included in each experiment. Standard curves obtained with the amplification of standard plasmids at increasing known concentrations were used to quantify TENM4 expression in different tissues.

Whole-cell patch clamp

Neurons or transfected N2a$^{Piezo1-/-}$ cells were immersed in an extracellular solution composed of (in mM): 140 NaCl, 4 KCl, 2 CaCl2, 1 MgCl2, 4 Glucose and 10 HEPES, pH adjusted to 7.4 with NaOH. For the MA-current analysis of the effects of PreScission on WT and *Tenm4*$^{KI/+}$ mice, neurons were immersed in the identical extracellular solution, supplemented with PreScission protease at a ratio of 2:1000 (v/v), 30 minutes prior to recordings. Patch pipettes (3-6 MΩ resistance) were fashioned from heat-polished borosilicate glass (Harvard apparatus, 1.17 mm x 0.87 mm) and filled with an intracellular solution containing (in mM): 110 KCl, 10 NaCl, 1 MgCl2, 1 EGTA, and 10 HEPES, with pH adjusted to 7.3 using KOH. Current-clamp experiments involved injecting steps of current in 50 pA increments from 0-950 pA to categorize sensory neurons into mechano- (large neurons) and nociceptors (small-medium neurons). Currents from neurons or transfected N2a$^{Piezo1-/-}$ cells were evoked using pillar deflection at a holding potential of -60 mV. Recordings were acquired with an EPC-10

amplifier with Patchmaster software (HEKA, Elektronik GmbH, Germany). For indentation experiments, neuronal cell membrane indentation in the range of 1 – 9 µm was achieved using a heat-polished borosilicate glass pipette (mechanical stimulator) manipulated by a MM3A micromanipulator. Bright field images were captured with a 40X objective and a CoolSnapEZ camera (Photometrics, Tucson, AZ) on a Zeiss 200 inverted microscope for the analysis of neuronal diameter. Currents and biophysical parameters were analyzed using FitMaster (HEKA, Elektronik GmbH, Germany).

Pillar arrays

Pillar arrays were prepared as described previously[4,6,46,58]. Briefly, salinized negative masters were used as templates. Negative masters were covered with degassed polydimethylsilozane (PDMS, syligard 184 silicone elastomer kit, Dow Corning Corporation) mixed with a curing agent at 10:1 ratio. After 30 min, glass coverslips were placed on the top of the negative masters containing 35 µm PDMS mix and baked at 110˚C for 60 min. The pillar arrays were peeled away from the master. The resulting dimensions of single pilus within the array was radius= 1.79 µm; length= 5.87 µm. While the elasticity was 2.1 MPa and the spring constant was 251 pN-nm as previously reported[4,6,46,58]. The pillar arrays were plasma cleaned (Deiner Electronic GmbH, Germany) and coated with PLL, subsequently N2a$^{Piezo1-/-}$ cells were cultured and were prepared as previously described. 24 hours after cells adherent on pillar, cells were transfected with either pRP TENM4-ALFA or pRK8 eGFP. After 24 hours of transfection, all cells were stained with FluoTag®-X2 anti-ALFA, as described earlier without fixation and Triton X-100. GFP cells or live-staining positive cells from respective cultures were selected for subsequent experiment.

To create quantitative data an individual pilus subjacent to the cell membrane was deflected using a heat-polished borosilicate glass pipette (approx. 2 mm in diameter) driven by a MM3A micromanipulator (Kleindiek Nanotechnik, Germany) as previously described

in[4,6,46,58]. Deflection stimuli were applied to a single pilus in the range of 1-1000 nm and cells were monitored using whole-cell patch-clamp. A bright-field image (Zeiss Axio Observer A1 inverted microscope) was taken before and during pillar deflection stimuli using a CoolSnapEZ camera (Photometrics, Tucson, AZ) and 40x objective. The pillar deflection was calculated by comparing the light intensity of the center of each pilus before and after the stimuli with a 2D-Gaussian fit (Igor Software, WaveMetrics, USA). Stimuli larger than 1000 nm were excluded.

Ex vivo skin nerve

Ex vivo skin nerve electrophysiology was performed on cutaneous sensory fibers of the tibial and saphenous nerves, following a previously established method[37]. Briefly, mice were euthanized by cervical dislocation, and the hair on the limb was shaved off. The hairy skin from the hind paw, along with the saphenous nerve up to the hip, was then dissected. The innervated hairy skin was placed in a bath chamber continuously perfused with warm (32°C) carbonated (95% O2, 5% CO2) interstitial fluid (SIF buffer): 123 mM NaCl, 3.5 mM KCl, 0.7 mM MgSO4, 1.7 mM NaH2PO4, 2.0 mM CaCl2, 9.5 mM sodium gluconate, 5.5 mM glucose, 7.5 mM sucrose, and 10 mM HEPES (pH 7.4). The skin was stretched and fixed “inside-out” using insect needles, allowing stimulation of the inner part of the skin with stimulator probes. For the glabrous skin, the tips of the toes were removed, and the skin was peeled back up to the ankle. The ankle was circumferentially cut, and the sciatic nerve was freed at hip level. The foot with the tibial nerve was placed in the organ bath chamber with superfused 30°C SIF buffer. Remaining muscle tissue, bones, and tendons were removed, and the skin was fixed in the "outside-out" configuration. The nerve was guided through a small opening to an adjacent chamber filled with mineral oil, where fine filaments were teased from the nerve and placed on a silver wire recording electrode.

Mechanically sensitive units were initially identified using blunt stimuli applied with a glass rod. Classification of mechanoreceptors was based on spike pattern and sensitivity to stimulus velocity, as described previously[18,19,37]. Raw electrophysiological data were recorded using a Powerlab 4/30 system and Labchart 8 software, with the spike-histogram extension supported by an oscilloscope for visual identification and subsequent analysis. All mechanical responses analyzed were adjusted for the latency delay between the electrical stimulus and the arrival of the action potential at the electrode.

Conduction velocity (CV) was measured using the formula CV = distance/time delay, where CVs > 10 m/s were classified as rapidly adapting mechanoreceptors (RAMs) or slowly adapting mechanoreceptors (SAMs), CVs < 10 m/s as Aδ fibers, and CVs < 1.5 ms/ as C-fibers.

Mechanically sensitive units were stimulated using a piezo actuator (Physik Instrumente (PI) GmbH & Co. KG, model P-841.60) connected to a force sensor with a calibrated conversion factor of Volts to Millinewtons. Various mechanical stimulation protocols were employed to identify and characterize sensory afferents. Vibrating stimuli with increasing amplitude and 20Hz frequency were applied to all types of mechanoreceptors, and the force required to evoke the first action potential was measured. A ramp and hold step with constant force (100 mN) was repeated with varying probe movement velocities (0.075, 0.15, 0.45, 1.5, and 15 mm s−1), and only firing activity during the dynamic phase was analyzed. SAM mechanoreceptors, Aδ mechanoreceptors, and nociceptors were mechanically tested with a constant ramp (1.5–2 mN m/s) and hold (10 seconds of static phase) stimulation, analyzing spikes evoked during the static phase. For electric search experimetns, data were collected from 5 *Tenm4*$^{fl/fl}$ (control) and 7 *Tenm4*^{CKO} mice and from 4 WT (control) and 5 *Tenm4*$^{KI/+}$ mice. For the stimulus-response-function recordings, data were collected from 4 WT and *Tenm4*$^{KI/+}$ mice and 6 *Tenm4*$^{fl/fl}$ and 9 *Tenm4*^{CKO} mice.

For the PreScission application, the five types of receptors are categorized into two main groups: mechanoreceptors (RA, SA, and D hairs) and nociceptors (AM and C fibers). Mechanoreceptors are subjected to a 20Hz step of increasing vibration amplitude applied at 30-second intervals, while nociceptors undergo a 150mM suprathreshold displacement at 30-second intervals. This protocol commences after isolating a receptive field with a metal ring. Prior to stimulation, it is crucial to verify the sealing status of the ring. The protocol involves stimulation for 3 minutes before applying the PreScission protease solution (concentration 20% (v/v) diluted in SIF). Stimulation is continued for an additional 45 minutes. At the end of the protocol, the conduction velocity is measured again to confirm the receptor's continued functionality. Experiments were conducted in a blinded manner (R.G. or M.A.K. were aware of the group allocations).

Electron microscopy

Saphenous nerves were dissected from four 12-week-old *Tenm4*^{CKO} and WT mice. The freshly isolated nerves were fixed in 4% paraformaldehyde/2.5% glutaraldehyde in 0.1 M phosphate buffer for 48 hours at 4°C. Following treatment with 1% OsO4 for 2 hours, each nerve underwent dehydration in a graded ethanol series and propylene oxide before being embedded in polyresin. Nerves were sectioned using a microtome into semi-thin (1μm) and ultrathin sections (70 nm). Semi-thin sections were stained with toluidine blue, and ultrathin sections were contrasted with uranyl acetate and lead acetate. Examination of semi-thin sections under a light microscope was performed to determine the total number of myelinated axons within the nerve. Ultrathin sections were examined using a Zeiss 910 electron microscope, and images were captured at an original magnification of 2500×. The A and C fiber dimensions were analyzed[46] using iTEM software.

Behavior

Von Frey filament testing was conducted to assess touch sensitivity in the mice. Animals were acclimated to the testing environment for two days in the week prior to the experiment. Paw withdrawal thresholds were then assessed using a standard Semmes-Weinstein set of von Frey filaments (ranging from 0.07 to 4 g, Aesthesio) in accordance with the up-and-down method[59]. The 50% paw withdrawal threshold was determined using the open source software, Up-Down Reader (https://bioapps.shinyapps.io/von_frey_app/)[60]. For the ascending dose-response experiments, von Frey filament testing involved assessing each filament five times and calculating the responses as proportions.

The cotton swab test measured sensitivity to gentle touch (0.7 – 1.6 mN), while brush testing evaluated dynamic mechanical sensitivity and measured intermediate touch sensation (>4 mN). A cotton swab (puffed out to approximately three times its original volume) and a soft brush (number 0) were applied to the plantar surface of the hind paw with gentle strokes. Each hind paw underwent testing three times, with a minimum interval of 5 minutes between consecutive tests. The number of withdrawals throughout the trials was counted and coded as a percentage of the total trials.

For Hargreaves assay, mice were acclimated for 30 minutes before the test. The infrared light source (Ugo Basile, 37370) was applied to the hind paw plantar surface, and withdrawal latency was automatically recorded. The focused radiant heat induced withdrawal within 10-15 seconds, with a 20-second cutoff to prevent tissue damage. The time required to withdraw the paws were recorded as indicators of their ability to assess temperature.

Sample sizes, described in each figure legend, were determined using GPower 3.1 software based on previous studies. No animals were excluded from the analysis. The mice were aged between 8 and 15 weeks old and were randomly assigned to various experimental groups, including control and other groups, ensuring a balanced representation across conditions. The experimenter was blinded to the group assignments during the von Frey filament testing.

Tripartite split-GFP complementation assay

The tripartite split-GFP complementation assay[61] was performed in HEK293T cells (ACC 635, DSMZ) cultured in DMEM (DMEM 41966) supplemented with 10% FCS and 1% Penicillin/Streptomycin. When HEK293T cells reached approximately 70% confluence, they were co-transfected with GFP1-9::iRFP702 (Addgene #130125), mouseTenms(N-terminus)-GFP10::mCHERRY, and mouseElkin1-GFP11::eBP2 plasmids using Fugene HD, following the manufacturer's instructions (Promega). Seven hours post-transfection, the culture medium was replaced with fresh medium. After 40 hours post-transfection, cells were fixed in 4% PFA, and images (eGFP, mCherry, and eBFP2) were acquired using cytationC10 (Biotek) with a 20x objective. Gen5 (Biotek) was used to analyze eGFP (interaction signal), mCherry (transfection signal of bait), and eBFP (transfection signal of prey) percentages of cells and fluorescence intensity. All signal intensities were normalized against background before color threshold overlapping for eGFP-positive (eGFP/mCherry) cell quantification.

Cellular co-localization assay

Transiently transfected N2a cells were imaged using an Airyscan fluorescence microscope (Axio, Zeiss) equipped with a ×63 1.4 NA oil lens. For cells transfected with either pRP TENM4-ALFA, pRK8 mScarlet-ELKIN1-EGFP, or mScarlet-PIEZO2, cells were prepared as previously described. After 48 hours of transfection, cells were fixed and stained with FluoTag®-X2 anti-ALFA, as described earlier. Cells were imaged in a total of four to five individual images under three experimental replicates. For each individual image, cells expressing both plasmids at similar expression levels were chosen and counted based on ALFA tag staining and mScarlet signals. The signal intensity in each group was normalized against control cells carrying only a single signal. The occurrence of normalized signals was

statistically analyzed using Manders' Overlap Coefficient (MOC) as a colocalized indication built into ZEN.

In vitro ALFA pull-down

HEK293T cells were transfected with either Full-length C-terminally ALFA-tagged TENM4 coupled with ELKIN1 or ALFA plasmid coupled with ELKIN1. Membrane protein complexes were solubilized from total lysates prepared from RIPA buffer (50 mM Tris, pH 7.5, 150 mM NaCl, 1.0% NP-40, 0.5% deoxycholate, 0.1% SDS, 3 mM DTT) with 1% DDM for 1 hour on ice. Both lysates were incubated with 20µL of ALFA SelectorPE resin for 1 hour at 4 °C on a roller drum. After washing in PBS containing 0.3% DDM, bound proteins were eluted under native conditions by sequentially incubating twice with 50µL PBS containing 200µM ALFA peptide for 30 minutes at 4°C. Samples corresponding to 1/500 of the input and 1/50 of eluate fractions were resolved by SDS–PAGE. Analysis was performed by Western blotting using a polyclonal rabbit-raised antibody against ELKIN1 and a polyclonal sheep-raised antibody against TENM4 (dilution 1:500), followed by HRP-conjugated goat anti-rabbit and anti-sheep IgG (Abcam Lot: GR288027-2, R&D Lot: 1522051, dilution 1:10,000). Blots were developed using the SuperSignal™ West Dura ECL Kit (Thermo Scientific) and imaged using a Bio-Rad ChemiDoc™ MP imaging system.

Microscopy setups

Epifluorescence images were obtained with an LSM880 Airyscan microscope (Carl Zeiss GmbH), equipped with a 63× NA1.4 oil immersion lens, and operated the Airyscan detector in super-resolution mode. This results in a pixel size of 35 nm. Excitation laser lines are 488, 561, and 680 nm. Independent tracks are used to switch between lines with a Z-stack according to the sample thickness in 0.2 um spacemen. Each line of the image is first scanned at 488 nm or 561 nm and subsequently at 561 nm. Pixel dwell times are adjusted to a value

between 1 and 2 microseconds with fourfold line averaging. After acquisition, Airyscan processing with default (=auto) parameters is employed, which results in a 16-bit image. This is stored in the proprietary CZI file format. data processing and signal quantification were performed using ImageJ.

Mass spectrometry analysis

The cell lines analysed were control Neuro2a cells or Neuro2a cells with a *Piezo1* genomic deletion as described previously[47]. The samples were lysed using 1% (w/v) sodium dodecyl sulphate and 1% (v/v) NP40, followed by SP3-bead-based digestion in an automated process utilising the AssayMAP Bravo robotic system (Agilent Technologies; adapted from[62]). In brief, protein lysates were treated with 5 mM dithiothreitol (DTT; Sigma-Aldrich) and heated to 90°C for 10 minutes for reduction. Alkylation was performed at room temperature with 10 mM iodoacetamide for 30 minutes, followed by quenching with 20 mM DTT for an additional 3 minutes. A mixture of 1 mg paramagnetic beads, comprising Sera-Mag Speed Beads, CAT# 09-981-121, and CAT# 09-981-123 (Thermo Fisher Scientific), was added, along with acetonitrile to a final concentration of 70% (v/v), and incubated for 18 minutes at room temperature. Beads were washed thrice with 200 µl 70% (v/v) ethanol, with 3-minute incubation at each step. Subsequently, 150 µl HEPES-KOH (pH 7.6) was added, followed by 4 µg of sequencing-grade LysC (Wako) and trypsin (Promega) for overnight incubation at 37°C. The supernatant was acidified with formic acid, and peptide solution was desalted using the AssayMap protocol. For reversed-phase liquid chromatography coupled to mass spectrometry (LC-MS) analysis, 1 µg of peptides per sample replicate was injected into an EASY-nLC 1200 system (Thermo Fisher Scientific) for separation employing a 110-minute gradient. Mass spectrometric measurements were conducted using an Exploris 480 (Thermo

Fisher Scientific) instrument operating in data-independent acquisition (DIA) mode. Raw files were analysed using DIA-NN version 1.8.1[63] in library-free mode, with an FDR cutoff of 0.01 and relaxed protein inference criteria whilst using the match-between runs option. Spectra were matched against a Uniprot mouse database (2022-03), including isoforms and a common contaminants database. Subsequent downstream analysis was performed using R version 4.3.2. MaxLFQ normalised protein intensities were log2 transformed and filtered to retain at least 4 valid values in at least one group for each protein before applying a downshift-imputation procedure. Significance determination utilised the limma package[64] to compute two-sample moderated t statistics, with nominal P-values adjusted using the Benjamini-Hochberg method.

Quantitative analysis of distinct peptides was conducted by utilising the report.tsv output generated by DIA-NN, followed by application of filtering criteria wherein peptides with Protein.Q.Value and Lib.Q.Value both less than or equal to 0.01 were retained for further analysis. Subsequently, the sum of the three most abundant fragments was computed for each precursor. The precursor with the highest abundance (Top1) was then selected for each distinct peptide sequence to facilitate peptide-level quantitation. Peptide maps were constructed by calculating position-based intensities, obtained by dividing the intensity of each peptide sequence by its respective length. In cases where multiple sequences of the same stretch were identified, intensities were aggregated to account for miscleavages or overlapping peptide sequences. Peptide intensities are not normalised. The mass spectrometry proteomics data have been deposited to the ProteomeXchange Consortium via the PRIDE[65] partner repository with the dataset identifier PXD050952.

<u>Statistical analysis</u>

Statistical analyses were performed using GraphPad Prism (version X). The study employed a variety of tests for different experimental assessments. Chi-squared and Fisher's exact tests evaluated proportions of neuron types, Mann-Whitney tests compared various responses, and Two-way repeated measures ANOVA with Sidak's post-test assessed stimuli-induced firing activity. Additionally, the impact of PreScission protease treatment was scrutinized with Friedman tests, Dunn's multiple comparisons tests, and Fisher's exact tests. The strength of interaction between ELKIN1 and TENM4 was determined via One-way ANOVA. A comprehensive statistical strategy, including Kruskal-Wallis tests, was implemented to analyze various datasets. Steps were taken to ensure that control and experimental groups were spread across different days to reduce bias.

Acknowledgement

This research was funded by an ERC grant to GRL (Sensational Tethers 789128) and from the Deutsche Forschungsgemeinschaft SFB958. A.T-L. H was a recipient for MOST postdoctoral research abroad program (111-2917-I-564-011). S.C. was a recipient of an Alexander von Humboldt research fellowship. We thank Maria Brauschweig, Franziska Bartelt, Kathleen Barda and Madlen Driesner for excellent technical assistance. Franziska Binder, Franziska Westphal, and Florian Keim for animal care taking. Séverine Kunz and Christina Schiel for electron microscopy and Protein Production & Characterization Technology Platform (MDC) team for excellent technical assistance. We thank members of Lewin lab for constructive discussions. We thank Stefan Lechner and Clément Verkest the mouse Piezo2-mScarlet construct.

Author contributions Conceptualization M.A.K., A.T-L. H and G.R.L. Mouse model selection, design and validation: G.R.L, V.B. and M.A.K; Patch clamp electrophysiology S.C (poking) and J.A.G-C. (Pillar array); Antibody validation MAK, L.D., R.G. and A.T-L.H;

Tripartite GFP design and implementation; candidate screening and molecular biology YASB, L.D and A.T-L. H. Skin nerve electrophysiology M.A.K, R.G, W.Z and G.R.L; Super resolution microscopy and biochemistry A.T-L. H; Behavioral assessments M.A.K. with R.G. Protein Production A.S. Proteomics J.A.G-C, S.C, O,P and P.M. Human skin samples S.H. Writing M.A.K. and G.R.L with input from all authors; Supervision and funding: G.R.L.

The authors declare no conflict of interest.

Extended Data Tables and Figures

TENM4 is an essential transduction component for touch and pain

Mohammed A. Khallaf[1,2], Angela Tzu-Lun Huang[1], Letizia Dalmasso[1], Sampurna Chakrabarti[1], Rowena Groeneveld[1], Yinth Andrea Bernal Sierra[1], Jonathan Alexis Garcia-Contreras[1], Anja Schütz[3], Valérie Bégay[1], Sarah Hedtrich[4,5,6,7], Wei Zhong[1], Oliver Popp[5], Philipp Mertins[5], and Gary R. Lewin[1,9,10*]

Gene	DRG		SCG	
	Mean	SEM	Mean	SEM
Adamts12	N.E.D		N.E.D	
Adamts20	0.163	0.069	0.068	0.037
Apc2	0.177	0.013	0.037	0.015
C3	0.232	0.021	0.3	0.018
Celsr1	0.464	0.071	0.401	0.04
Clstn2	0.673	0.034	0.276	0.08
Coagulaion factor8	0.387	0.012	0.09	0.041
Col5a1	N.E.D		0.469	0.158
Dmbt1	N.E.D		N.E.D	
Fbn2	0.322	0.085	0.308	0.038
Frem2	0.362	0.062	N.E.D	
Igsf10	0.482	0.044	0.336	0.006
Madd	0.405	0.151	0.391	0.119
Notch3	0.602	0.072	0.309	0.023
Pcnxl3	0.595	0.217	0.439	0.022
Pcsk5	0.388	0.325	N.E.D	
Pkhd1l1	0.361	0.008	0.109	0.016
Plxnb1	0.66	0.053	0.541	0.002
RIKEN 672066o15	0.823	0.137	0.34	0.049
4931403E03Rik	0.103	0.016	0.178	0.028
5430411K18Rik	0.497	0.071	0.359	0.041
Robo1	0.414	0.069	0.378	0.102
Scrib	0.188	0.066	N.E.D	
Slit1	0.234	0.025	N.E.D	
Slit2	0.568	0.043	0.23	0.07
Stab1	0.519	0.034	0.482	0.019
Strc3	N.E.D		N.E.D	
Svep1	0.572	0.01	0.36	0.178
Tecta	0.287	0.041	N.E.D	
Tenm1	0.718	0.111	0.398	0.186
Tenm2	0.656	0.01	0.526	0.19
Tenm3	0.686	0.048	0.51	0.076
Tenm4	0.28	0.059	N.E.D	
Thsd7a	0.992	0.049	0.995	0.01

Extended Data Table 1: 34 extracellular proteins with furin cleavage sites.

A bioinformatics approach identified 11,302 mouse genome proteins with at least one furin cleavage site RX(K/R)R. Using DAVID, these proteins were categorized by extracellular matrix localization, sequence size, and DRG expression patterns via GenePaint[24], revealing 33 proteins with DRG staining signals. Six proteins (highlighted in yellow) were chosen as promising candidates for their specificity to DRG.

Accession	Description	Size (aa)	DRG expression
8AQT_A	Chain A, Processed angiotensin-converting enzyme 2,Ig gamma-2A chain C region, membrane-bound form	886	No
8AQW_A	Chain A, Processed angiotensin-converting enzyme 2,Ig gamma-2A chain C region, A allele	884	No
7XMS_S	Chain S, Signle chain viable fragment of antibody	292	Not available
6NJL_K	Chain K, 15F1 Fab heavy chain	262	Not available
5ZRY_A	Chain A, Ankyrin repeat and SAM domain-containing protein 1A,Ephrin type-A receptor 6	194	Yes
6TFB_A	Chain A, Frizzled-8	138	Yes

Extended Data Table 2

Extracellular proteins with a consensus PreScission cleavage site.

Using a peptide search of the mouse proteome we found six proteins were detected with at least one PreScission consensus cleavage site LEVLFQ/GP.

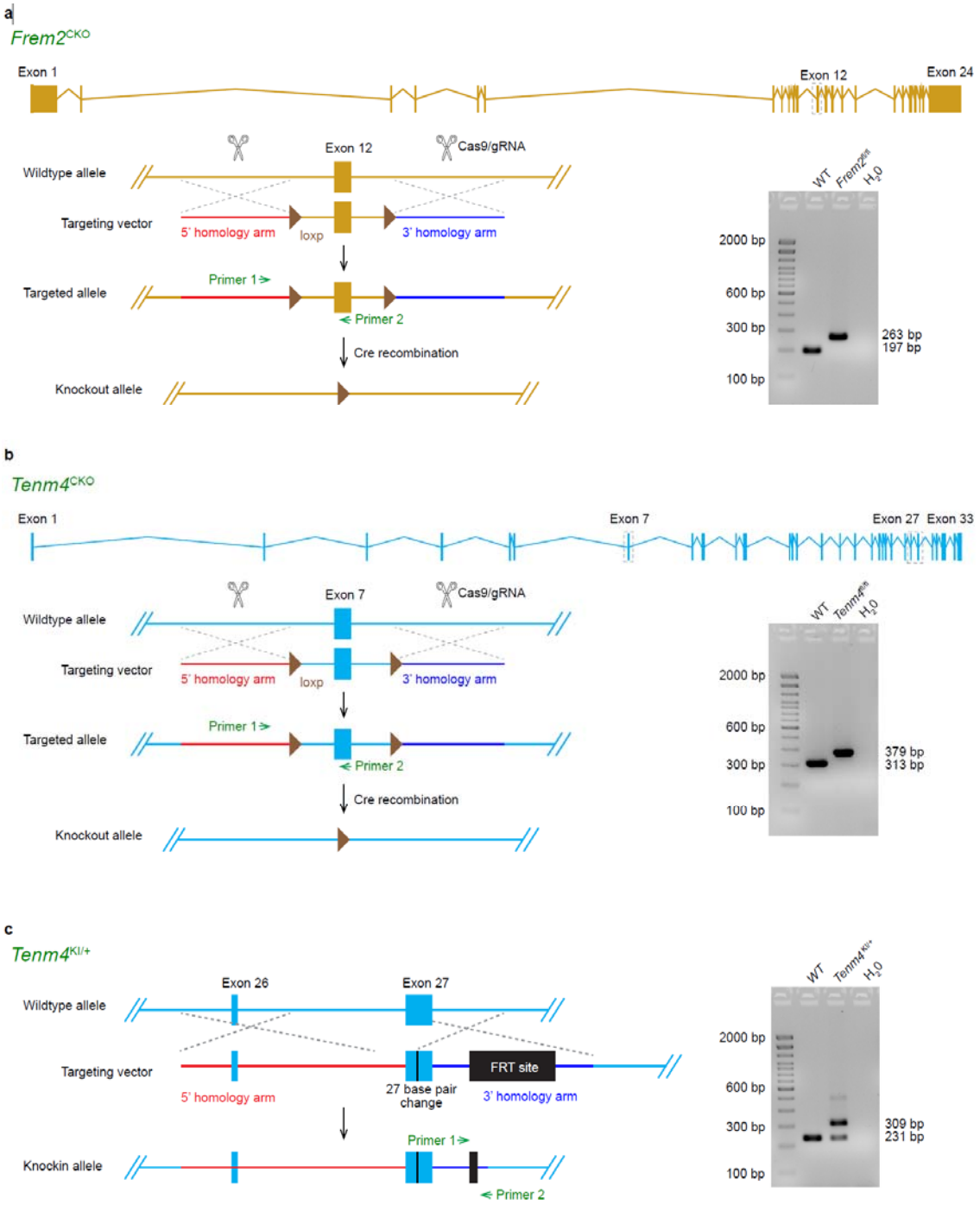

Extended Data Fig. 1

Strategies of generating transgenic mice. a. Schematic of the *Frem2*^{CKO} mouse model targeting strategy using a targeting vector constructed with Infusion technology. The plasmid structure includes a 5' homologous arm (3.0kb), a Loxp sequence (1.0kb), and a 3' homologous arm (3.0kb). Right, PCR bands from genomic DNA of WT, *Frem2*$^{fl/fl}$ are presented. **b**. Diagram depicting *Tenm4*^{CKO} mouse model creation with an Infusion-constructed targeting vector (5' homologous arm: 3.0 kb, flox: 0.9 kb, 3' homologous arm: 3.0 kb), along with PCR bands from genomic DNA of WT and *Tenm4*$^{fl/fl}$ mice. **c**.

Diagram illustrating the creation of the *Tenm4* $^{KI/+}$ mouse model using using homologous recombination in ES cells. The targeting vector was designed to introduce a 21 bp change in exon 27 of Tenm4 (5' homologous arm: 7.9 kb, and 3' homologous arm: 2.5 kb). The Neo selection cassette, flanked by FRT sites, is inserted. FLP recombinase in the built-in FLP ES cell line led to Neo cassette excision, leaving one FRT site (78 bp), which was used as a marker for a successful event. On the right, PCR bands from genomic DNA of WT and *Tenm4* $^{KI/+}$ mice are displayed.

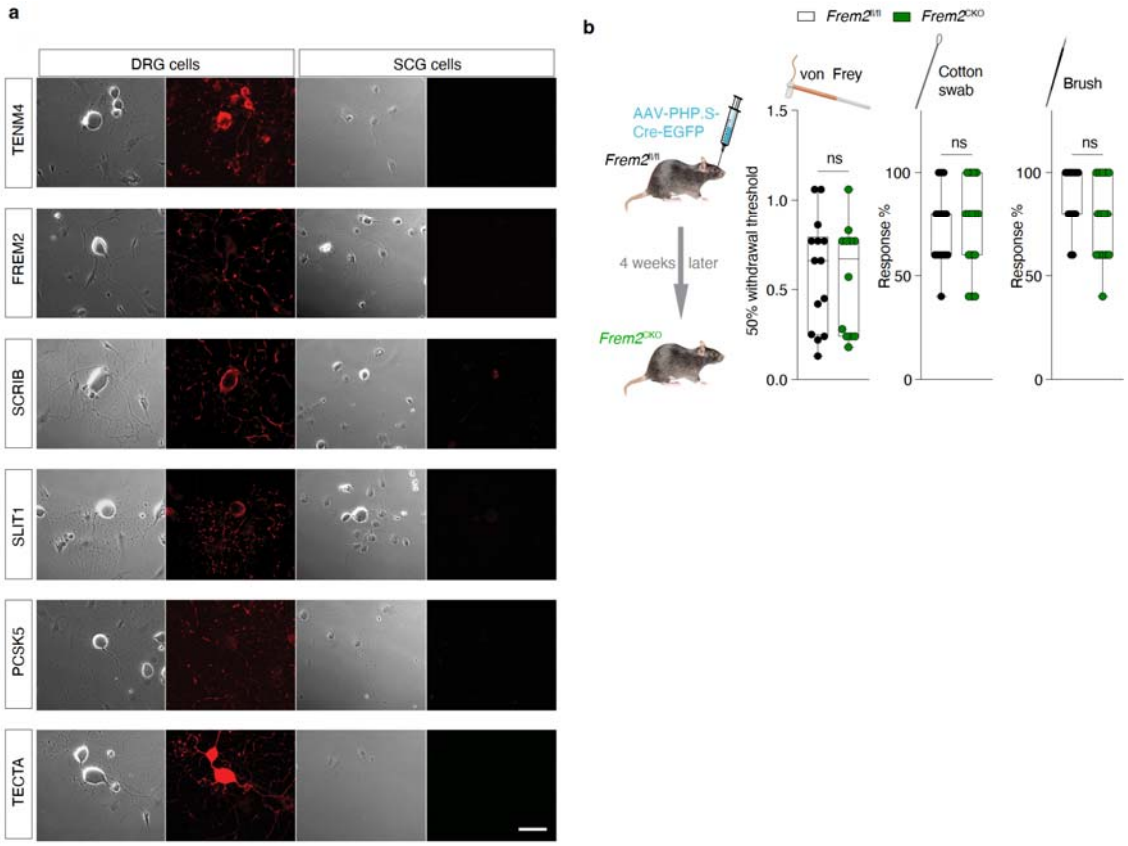

Extended Data Fig. 2

Candidate screening a. The 6 tether protein candidates exhibit a patchy-like expression pattern in the neurites of DRG cells, and no staining was observed in the non-mechanosensitive SCG cells cultured on plates coated with laminin. Scale bar is 10µm. **b**. Left, a diagram depicting generation of *Frem2*^{CKO} mice via retro-orbital injection of AAV-PHP.S-Cre-EGFP in the sinus of *Frem2*$^{fl/fl}$ mice. Right, *Frem2*^{CKO} mice exhibit normal touch sensitivity compared to the control *Frem2*$^{fl/fl}$ mice.

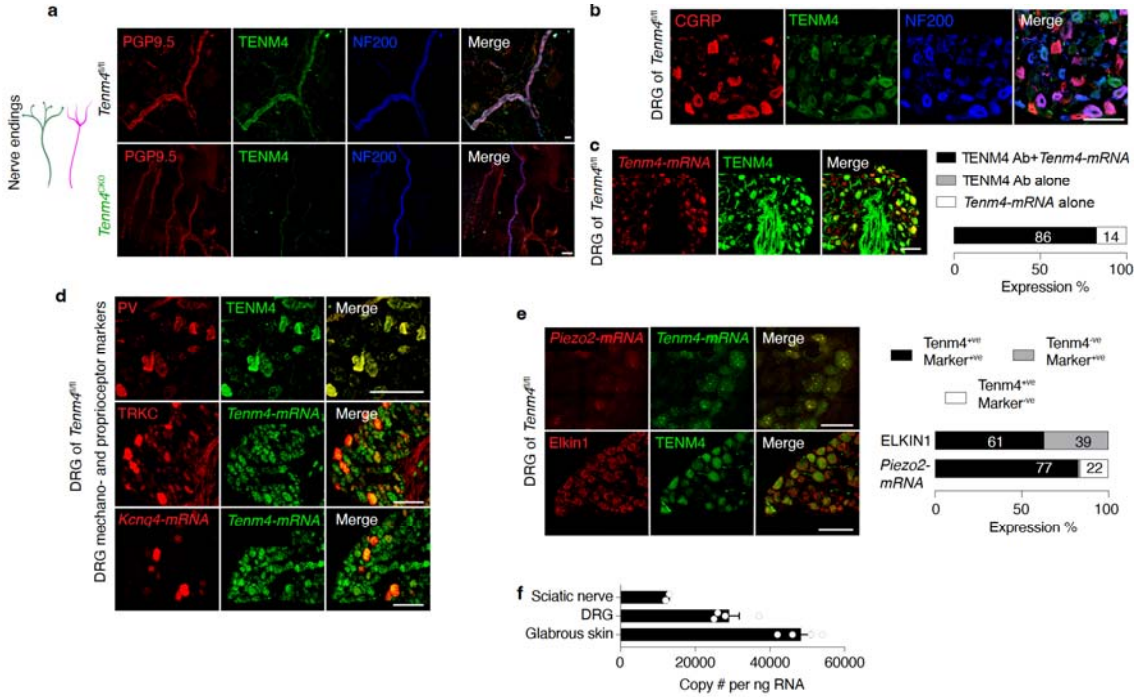

Extended Data Fig. 3

***Tenm4* is expressed in cutaneous mechanoreceptors. a**. TENM4 positive staining found in nerve endings (in hairy skin), visualized by PGP9.5 (a neuronal marker) and NF200 in WT mice (top panels). *Tenm4*^{CKO} mice exhibit a notable decrease in TENM4+ sensory nerve endings (below panels). Scale bar 20µm. **b**. Representative images highlighting the enrichment of TENM4 in DRG neurons positive for NF200 and CGRP (a marker of peptidergic neurons). Scale bar is 50µm. **c**. Left, representative images demonstrate the colocalization of a smFISH probe targeting Tenm4 mRNA with the TENM4 antibody staining. Right, quantification of TENM4+ sensory neurons stained with both the smFISH probe and the antibody. Scale bar is 100µm. Quantification in each group from 2 male and 3 female mice; more than 700 neurons were counted in each group. **d**. Representative images highlighting the enrichment of TENM4 in DRG neurons positive for mechanoreceptors and proprioceptors markers. Scale bar is 100µm. **e**. Left, representative images highlighting the enrichment of TENM4 in DRG neurons positive for neuronal marker (PGP9.5) and ion channel markers (Piezo2 and Elkin1). Scale bar is 100µm. Right, quantification of TENM4+ sensory neurons co-labeled with neuronal and ion channels markers. Quantification in each group from 2 male and 3 female mice; more than 700 neurons were counted in each group. **f**. Quantification of *Tenm4* mRNA expression level (copies of transcript per ng total RNA) in skin, DRG, and sciatic nerve. Quantification in each group from 2 male and 2 female mice.

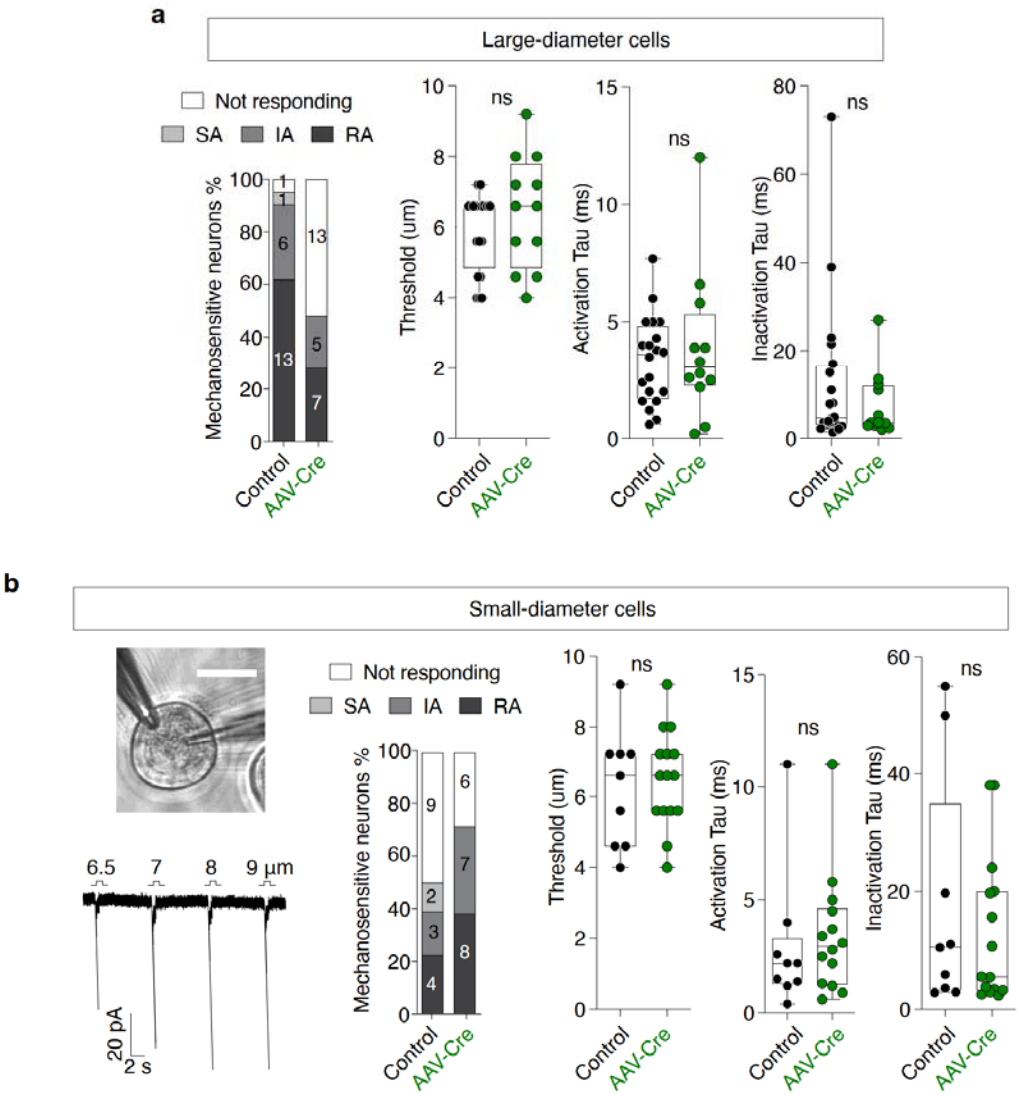

Extended Data Fig. 4

Mechanically activated current kinetics in *Tenm4*^{CKO} mice. a. Large-diameter neurons from both *Tenm4*$^{fl/fl}$ and *Tenm4*^{CKO} mice exhibited similar number of cells displaying rapidly, intermediate, and slowly adapting MA-currents, mechanical thresholds, as well as activation and inactivation kinetics. **b**. Representative traces of poking-induced currents resulting from indentations ranging between 1 and 9µm on GFP+ large-diameter neurons in *Tenm4*^{CKO} mice. Small-diameter neurons from both *Tenm4*$^{fl/fl}$ and *Tenm4*^{CKO} mice exhibited similar number of cells displaying rapidly, intermediate, and slowly adapting MA-currents, mechanical thresholds, as well as activation and inactivation kinetics. Chi-squared test and Mann-Whitney test; ns indicates $p > 0.05$. Data were collected from 5 *Tenm4*$^{fl/fl}$ and 5 *Tenm4*^{CKO} mice. Means ± s.e.m.

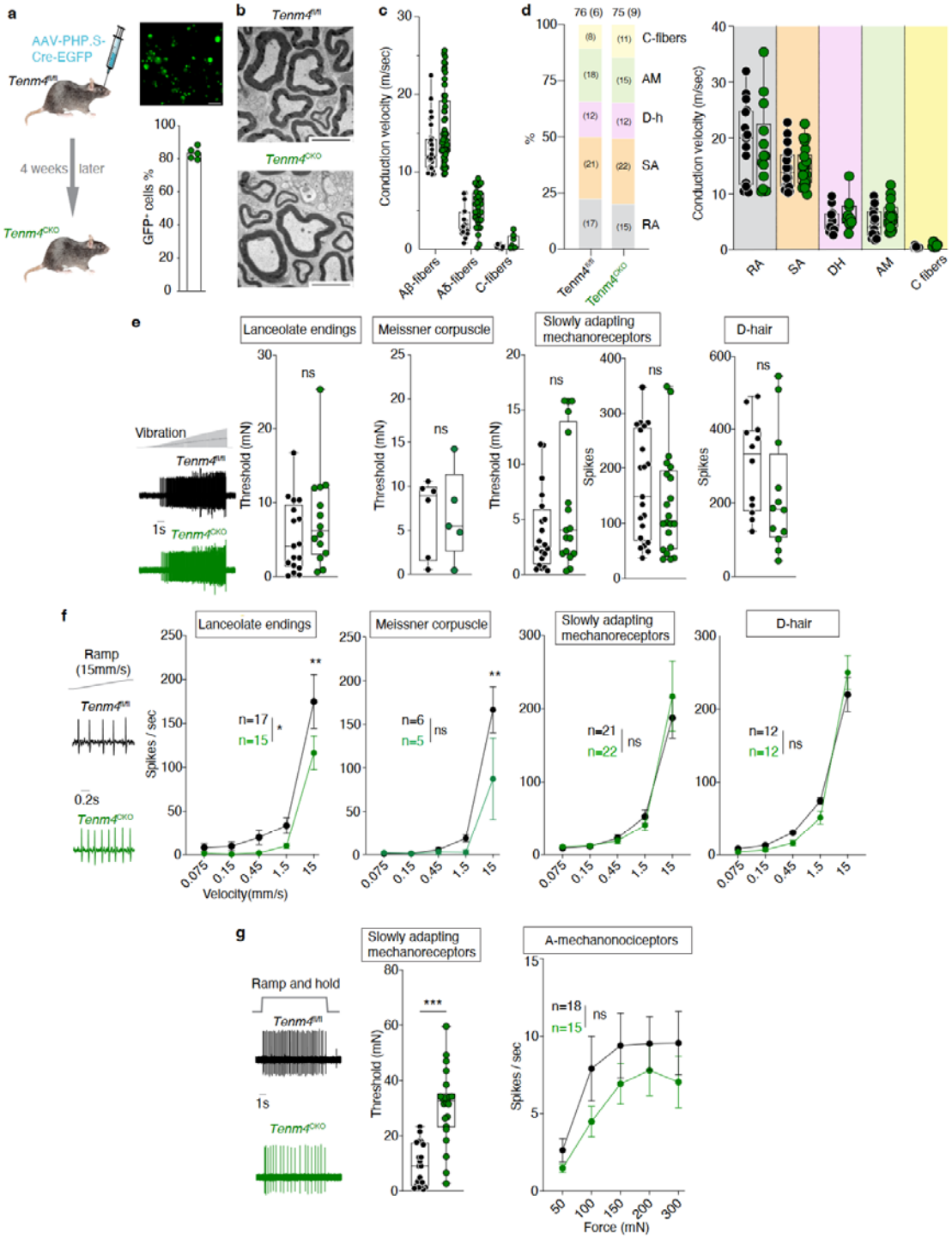

Extended Data Fig. 5

Stimulus-response functions after *Tenm4* gene deletion. a. Left, schematic for generation of *Tenm4*^{CKO} mice via retro-orbital injection of AAV-PHP.S-Cre-EGFP of *Tenm4*$^{fl/fl}$ mice. Top right, Representative image of DRG sensory neurons from *Tenm4*^{CKO} mice 4 weeks after being transduced with AAV-PHP.S-Cre-EGFP. Scale bar is 50 µm. Bottom right, quantification of the percentage of GFP positive cultures DRG neurons after viral transduction. Dots represent 4 dishes from 3 mice. **b**.

Example electron-micrographs from the saphenous nerve of a *Tenm4*$^{fl/fl}$ (top) and *Tenm4*^{CKO} mouse (bottom). Scale bar is 20μm. **c**. Conduction velocities of sensory afferents recorded from 6 *Tenm4*$^{fl/fl}$ and 9 *Tenm4*^{CKO} mice. **d**. Proportions and conduction velocities of different sensory afferents recorded from 6 *Tenm4*$^{fl/fl}$ and 9 *Tenm4*^{CKO} mice. **e**. Example traces of single sensory units from control and *Tenm4*^{CKO} mice responding to a linearly increasing 20Hz sinusoidal force stimulus. The firing frequency for RAMs in hairy skin or those innervating Meissner's corpuscles and Merkel cells, as well as the mechanical threshold of Merkel cells and D-hairs, showed no significant difference between *Tenm4*$^{fl/fl}$ and *Tenm4*^{CKO} mice. Mann-Whitney test; ns indicates $p > 0.05$. Data were collected from 6 *Tenm4*$^{fl/fl}$ and 9 *Tenm4*^{CKO} mice. **f**. Example traces of single sensory units from *Tenm4*$^{fl/fl}$ and *Tenm4*^{CKO} mice responding to a ramp stimulus with a 15 mm/sec movement velocity. The firing activity of sensory afferents innervating Merkel cells and D-hairs, in response to varying movement velocities, showed no significant differences between *Tenm4*$^{fl/fl}$ and *Tenm4*^{CKO} mice. Two-way repeated measures ANOVA followed by Sidak's post-test; ns indicates $p > 0.05$. Data represent the mean ± s.e.m and were collected from 6 *Tenm4*$^{fl/fl}$ and 9 *Tenm4*^{CKO} mice. **g**. Example traces of single sensory afferents innervating Aδ mechanonociceptors in in *Tenm4*$^{fl/fl}$ and *Tenm4*^{CKO} mice responding to a ramp-and-hold stimulus with a constant force of 100mN. The mechanical threshold and firing activity of various sensory afferents showed no significant difference between *Tenm4*$^{fl/fl}$ and *Tenm4*^{CKO} mice. Mann-Whitney test and Two-way repeated measures ANOVA followed by Sidak's post-test; ns indicates $p > 0.05$. The line graph represents the mean ± s.e.m. and were collected from 6 *Tenm4*$^{fl/fl}$ and 9 *Tenm4*^{CKO} mice.

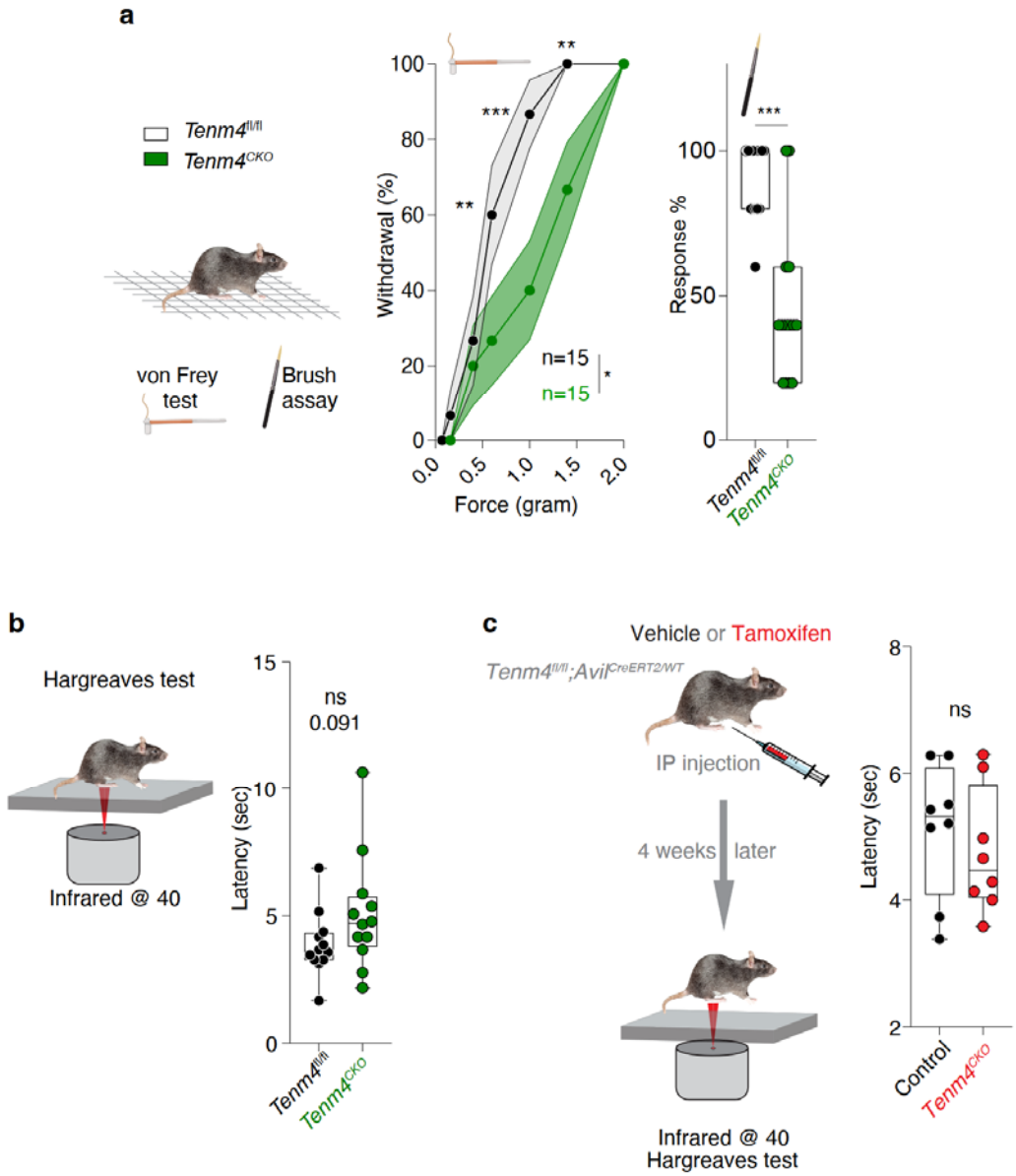

Extended Data Fig. 6

***Tenm4^{CKO}* mice display mechanosensory deficits but normal responses noxious heat. a.** Responses to an ascending series of von Frey hair stimuli and brush reponses in *Tenm4^{CKO}* mice. The line graph illustrates the mean represented by points and the surrounding shades indicate s.e.m. **b**. Left, a Hargreaves test schematic for paw withdrawal latency, indicating thermal pain thresholds. Right, *Tenm4^{CKO}* mice showed comparable responses to heat stimulus, similar to *Tenm4$^{fl/fl}$* mice. **c**. Left, a diagram illustrating the generation of *Tenm4^{CKO}* and control mice via tamoxifen injections in *Tenm4l$^{fl/fl}$;Avil$^{CreERT2/WT}$* mice. Right, *Tenm4^{CKO}* mice showed comparable responses to heat stimulus, similar to the control mice. Mann-Whitney test; ns indicates $p > 0.05$. Data were collected from 12 (a), 8 (b), animals per group. Means ± s.e.m.

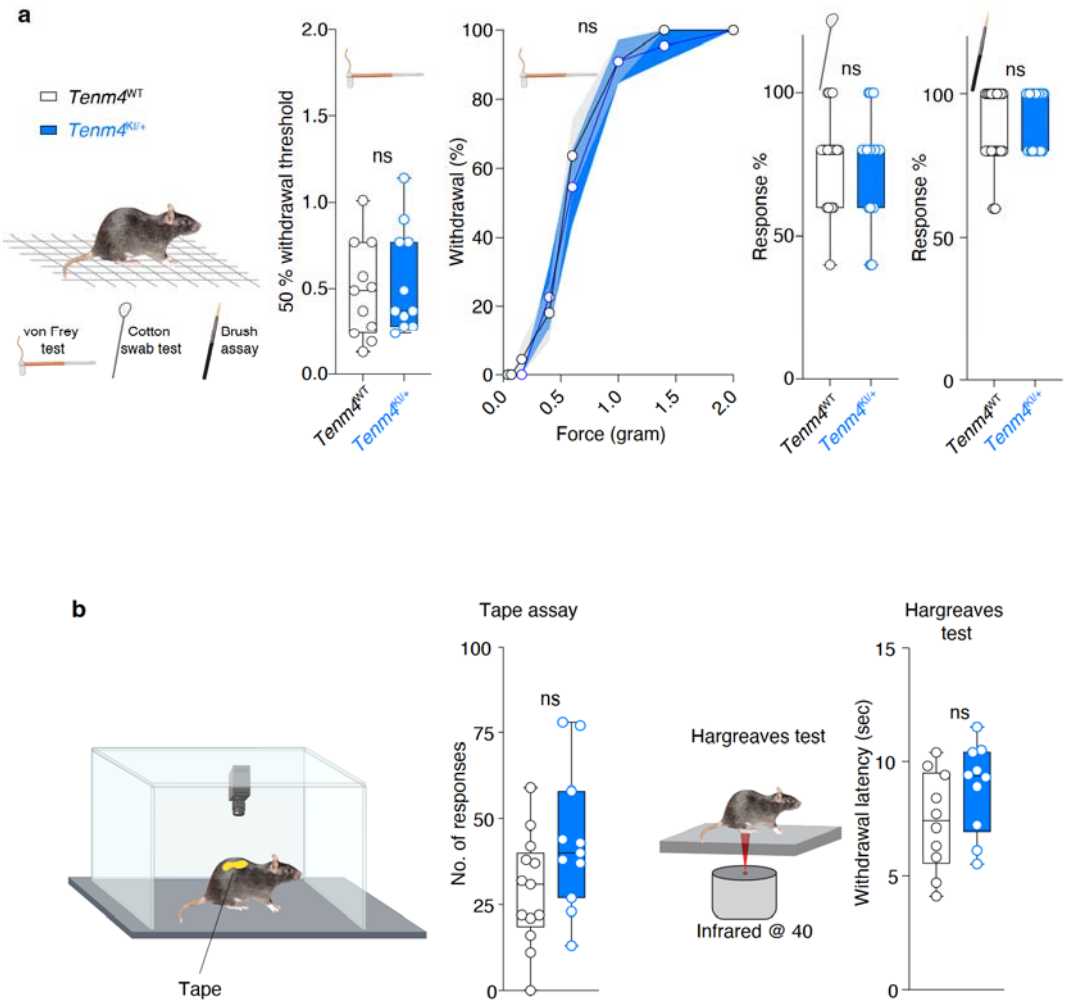

Extended Data Fig. 7

Behavioral characterization of *Tenm4*$^{KI/+}$ mice. a. *Tenm4*$^{KI/+}$ mice exhibited similar withdrawal thresholds and responses to von Frey filaments, a cotton swab, and dynamic brush, compared to wildtype mice. **b**. *Tenm4*$^{KI/+}$ mice display normal responses to tape and heat stimuli, similar to WT mice. Mann-Whitney test and Two-way repeated measures ANOVA followed by Sidak's post-test; ns indicates $p > 0.05$. Data were collected from 11 (von Frey, cotton swab and brush tests), 13 (tape assay) and 10 (Hargreaves test) mice in each category. The line graph represents the mean ± s.e.m.

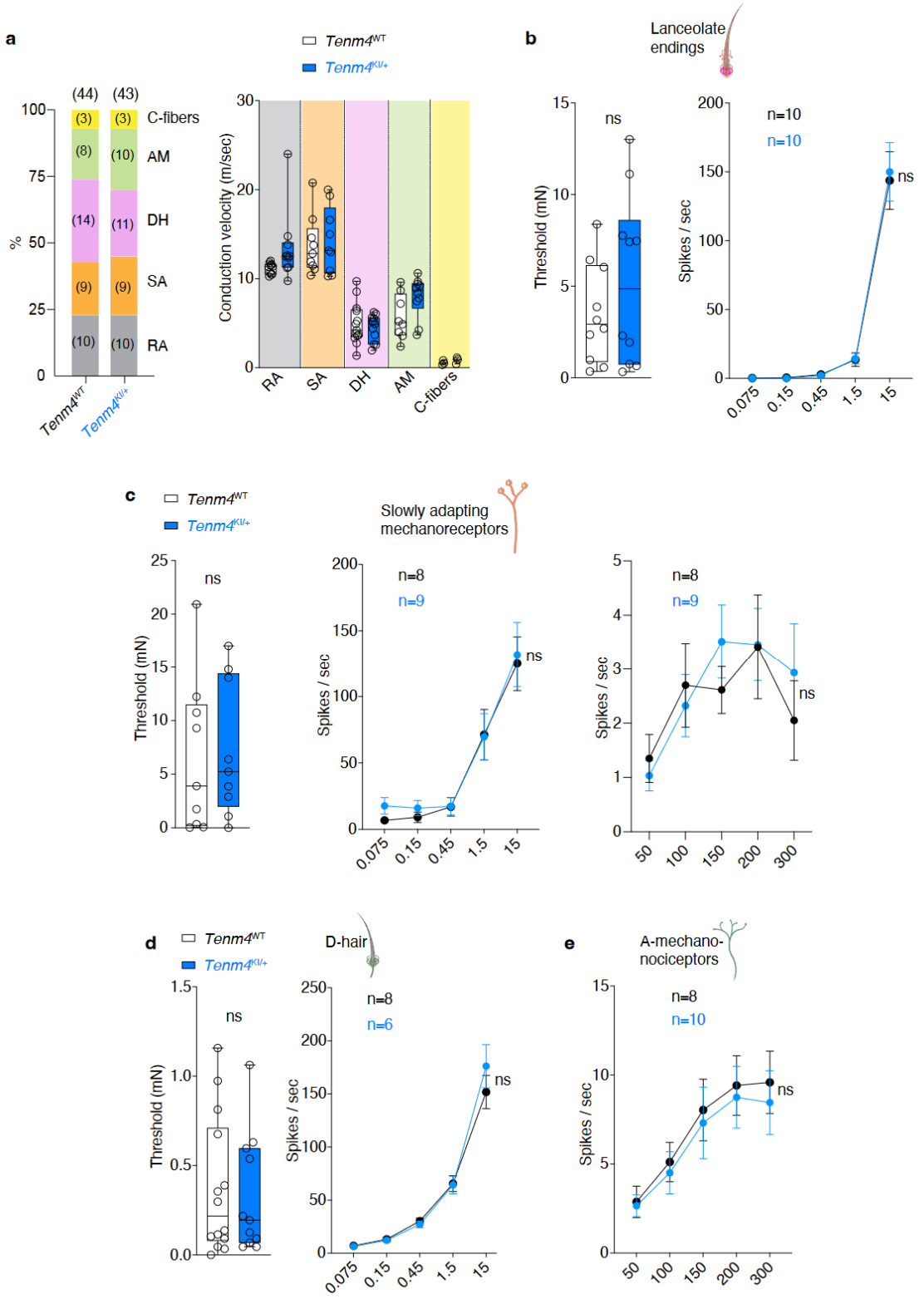

Extended Data Fig. 8

Electrophysiological characterization of *Tenm4*$^{KI/+}$ mice. a. Proportions and conduction velocities of different sensory afferents recorded from 5 WT and 4 *Tenm4*$^{Pres.KI/+}$ mice show no marked changes.
1380 **b**. The mechanical threshold and firing activity during the dynamic phase of ramp stimuli showed no

significant differences between RAMs in WT and *Tenm4*$^{KI/+}$ mice. **c**. The mechanical threshold firing activity during the dynamic phase of ramp stimuli, as well as the static phase of ramp-and-hold stimuli, showed no significant differences between SAMs in WT and *Tenm4*$^{Pres.KI/+}$ mice. **d**. The mechanical threshold and the firing activity during the dynamic phase of ramp stimuli showed no significant differences between D hairs receptors in WT and *Tenm4*$^{Pres.KI/+}$ mice. **e**. The firing activity during the static phase of ramp-and-hold stimuli, showed no significant differences between Aδ mechanonociceptors in WT and *Tenm4*$^{Pres.KI/+}$ mice. Mann-Whitney test and Two-way repeated measures ANOVA followed by Sidak's post-test; ns indicates $p > 0.05$. Data were collected from 5 WT and 4 *Tenm4*$^{Pres.KI/+}$ mice. Means ± s.e.m.

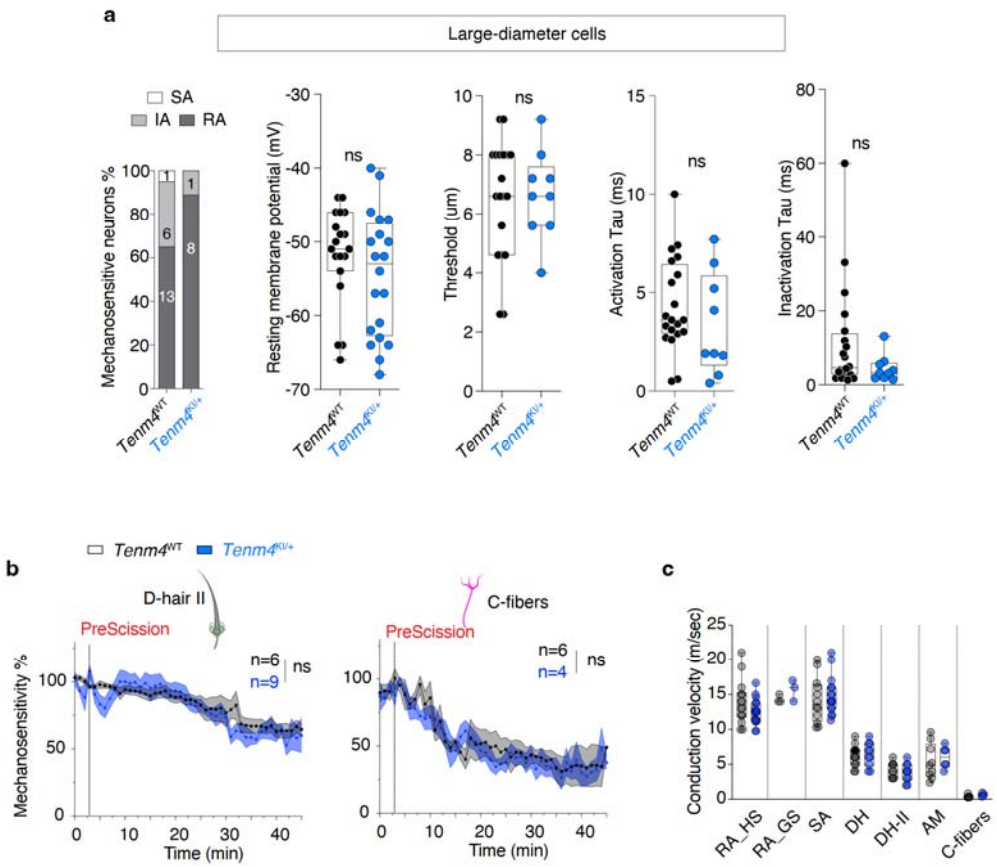

Extended Data Fig. 9

Lack of PreScission effects on C-fiber nociceptors a. Large-diameter DRG neurons from PreScission-treated WT and PreScission-treated *Tenm4*$^{Pres.KI/+}$ mice exhibited similar percentages of rapidly, intermediate, and slowly adapting MA-currents, mechanical thresholds, as well as activation and inactivation kinetics. **b**. Individual sensory fibers innervating D hairs (with slow conduction velocities; see following panel) and C-fibers in WT and *Tenm4*$^{KI/+}$ mice retain functionality after exposure to PreScission protease applied to their receptive fields. **c**. Conduction velocities of sensory afferents recorded from 26 WT and 23 *Tenm4*$^{Pres.KI/+}$ mice. D-hairs were classified to two categories based on their conduction velocities. D-hair II units had slower conduction velocities and seemed insensitive to the PreScission protease.

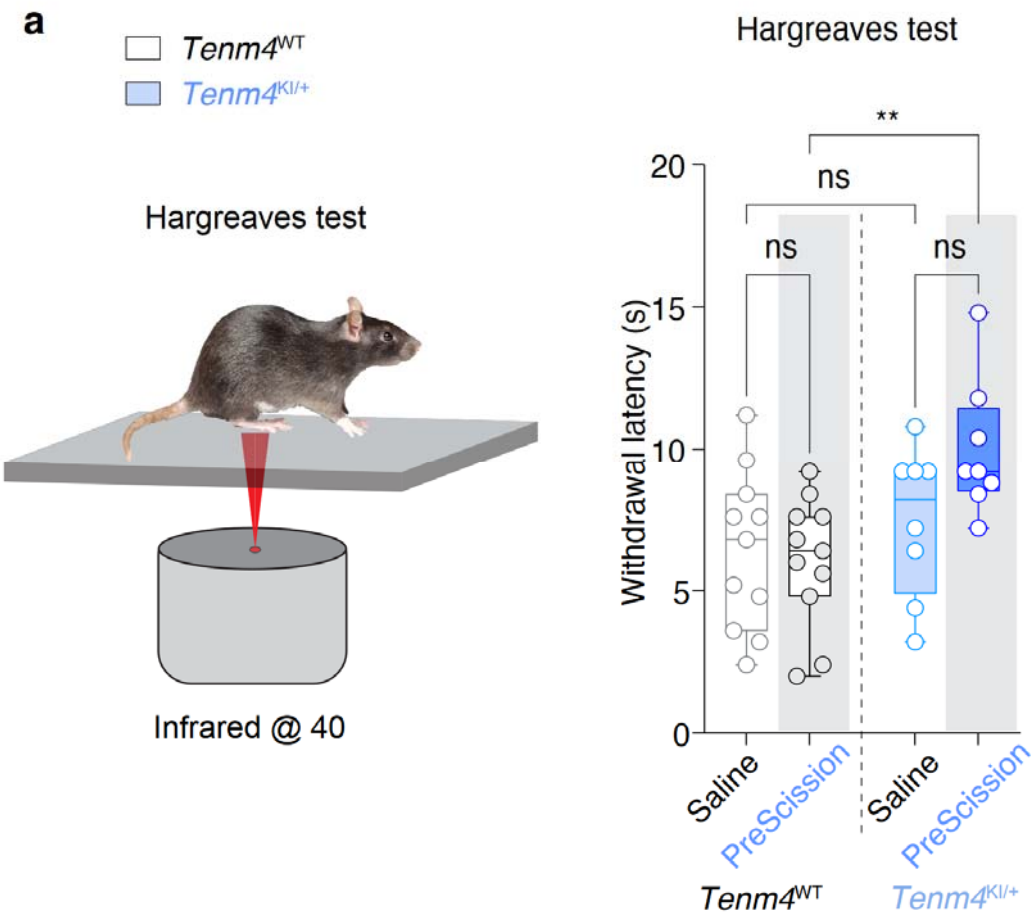

1405 **Extended Data Fig. 10**

Tenm4 cleavage may slightly alter sensitivity to thermal stimuli. a. Left, Schematic of the Hargreaves test Right, *Tenm4*$^{KI/+}$ mice injected with PreScission showed slightler longer withdrawal latencies (i.e., decreased responses) to heat stimulus, compared to PreScission-injected WT mice. Data were collected from 11 WT and 8 *Tenm4*$^{Pres.KI/+}$ mice. Two-way repeated measures ANOVA
1410 followed by Sidak's post-test; ns indicates $p > 0.05$; ** indicates $p < 0.01$.

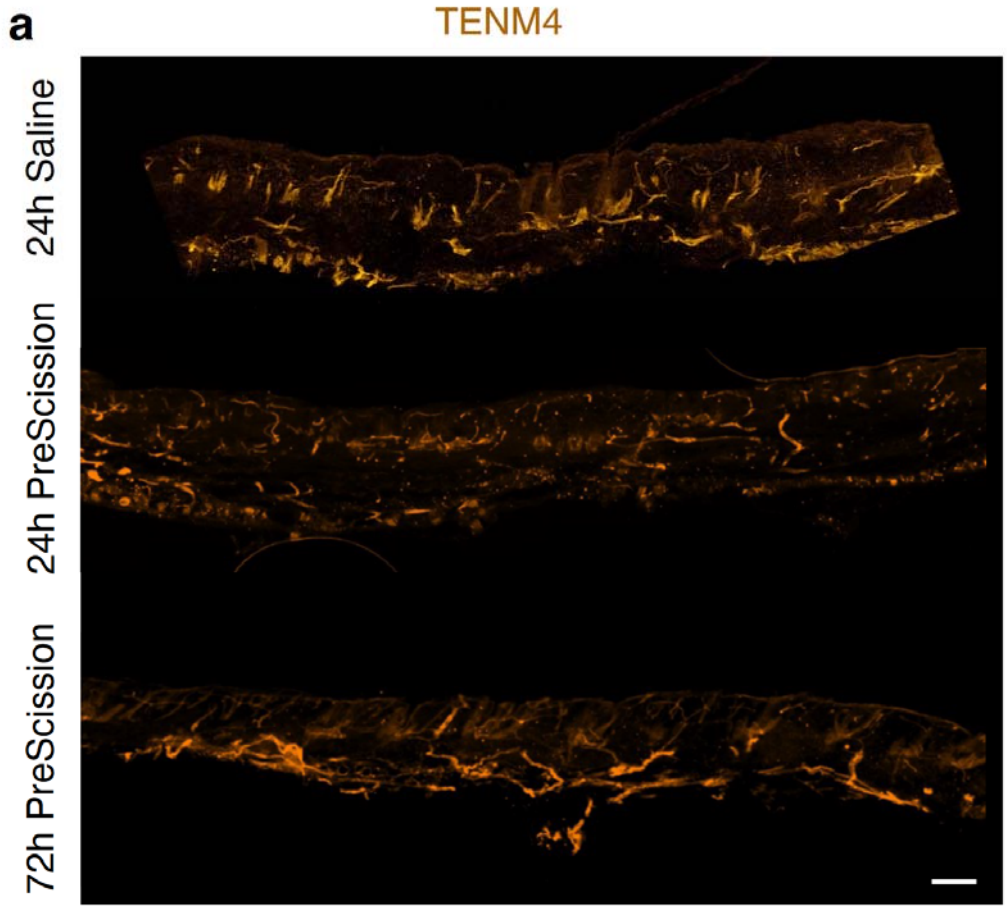

Extended Data Fig.11

1415 **TENM4 labelling signal recovers 72 hours after PreScission injection.**

a. Representative images after 24 and 72 hours from PreScission protease, or 24 hours from vehicle (NaCl) injection into the hairy skin in *Tenm4*$^{Pres.KI/+}$ mice. TENM4-expressing fibers became barely detectable at 24 hours but recover by 72 hours from PreScission protease in *Tenm4*$^{Pres.KI/+}$ mice.

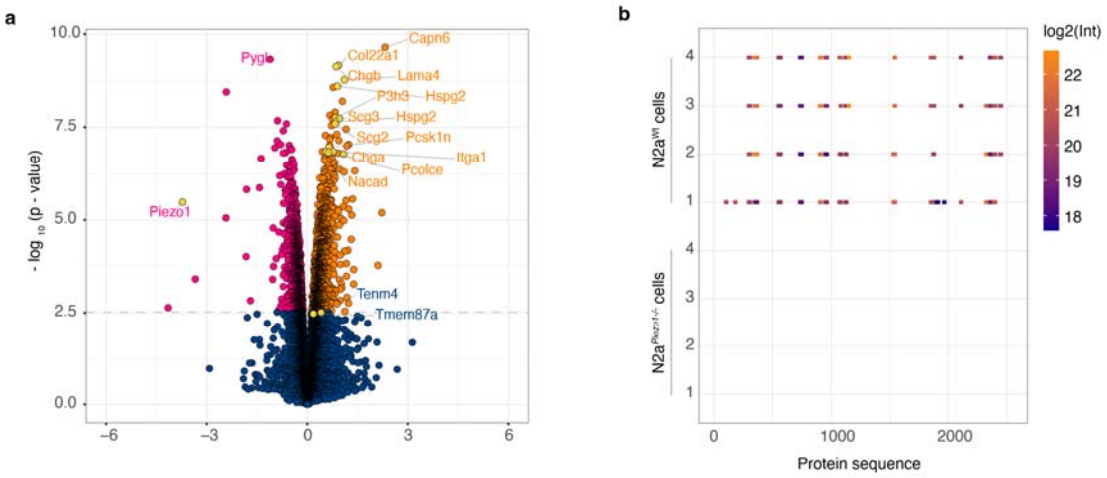

Extended Data Fig. 12

Proteomic profile of N2a cells and N2a$^{\text{Piezo1-/-}}$ cells. **a**. Volcano plot of mass spectrometry analyses of N2a$^{\text{Piezo1-/-}}$ compared to WT N2a cells (n = 4). Both Elkin1 (Tmem87a) and TENM4 were endogenously expressed in N2a cells and both were slightly upregulated upon Piezo1 gene deletion. Many of the proteins extensively upregulated in N2a$^{\text{Piezo1-/-}}$ N2a cells (highlighted in the plot) are involved either in the organization of the extracellular matrix (ECM) or in the regulation of the secretory granules, suggesting a link between mechanosensitivity and ECM composition. **b** Peptide map shows local peptide coverage of PIEZO1 across all WT and N2a$^{\text{Piezo1-/-}}$ samples. Displayed values are in linear space whilst a log2 transformation is applied to the color scheme.

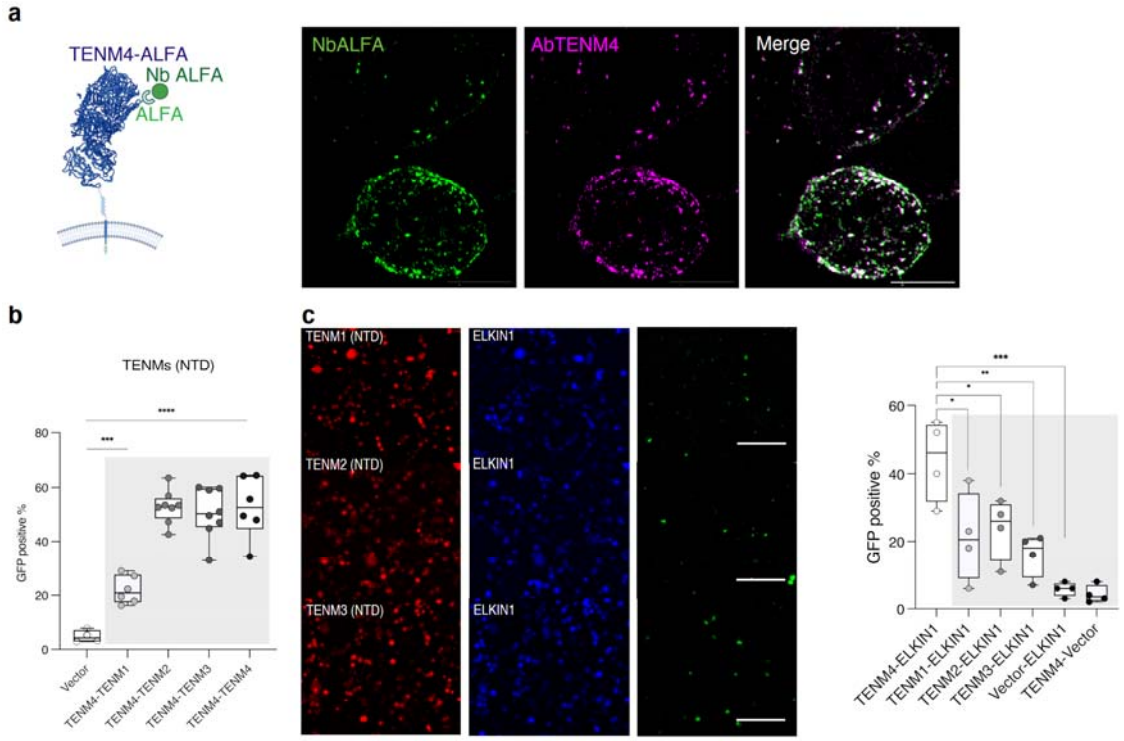

Extended Data Fig. 13

Homo and Heterologous interactions between the Teneurins a. Schematic of ALFA tagged TENM4. Note the ALFA epitope should be recognized by nanobodies (NbALFA) without the need to permeabilize the cells. **b**. N2a cells transfected with TENM4-ALFA and stained with NbALFA labeled with AbberiorStar635P (NbALFA-Ab635P, green) and our anti-TENM4 C-terminal antibody (purple). Note the clear colocalization of the two signals. **c.** Quantification of the GFP-complementation signal in the split-GFP assay. Assay confirms heterologous interactions between the Teneurins. Pair wise interactions tested with TENM4(NTD) between TENM1(NTD), TENM2(NTD), TENM3(NTD) and TENM4(NTD). **d**. Representative images depicting the tripartite-GFP interaction between ElKIN1 and other Teneurins N-terminals (TENM1 (NTD), TENM2 (NTD), or TENM3 (NTD)). Scale bar is 100μm. Quantification shown in Fig. 6.